Aus der Poliklinik für Zahnerhaltung und Parodontologie

Klinikum der Ludwig-Maximilians-Universität München

Einsatz der Magnetresonanztomographie für die Detektion periapikaler Entzündungsprozesse und assoziierter mukosaler Pathologien

Dissertation
zum Erwerb des Doktorgrades der Humanbiologie
an der Medizinischen Fakultät der
Ludwig-Maximilians-Universität München

vorgelegt von

Priv.-Doz. Dr. med. Dr. med. dent. Egon Burian, MBA

aus

Reschitz/ Rumänien

Jahr

2024

Mit Genehmigung der Medizinischen Fakultät der
Ludwig-Maximilians-Universität zu München

Erster Gutachter:	Prof. Dr. med. Dr. med. dent. Matthias Folwaczny
Zweiter Gutachter:	Priv.-Doz. Dr. rer. nat. Uwe Baumert
Dritter Gutachter:	Prof. Dr. med. dent. Daniel Edelhoff
Dekan:	Prof. Dr. med. Thomas Gudermann
Tag der mündlichen Prüfung:	15.01.2024

Affidavit

LMU LUDWIG-MAXIMILIANS-UNIVERSITÄT MÜNCHEN | Promotionsbüro Medizinische Fakultät | MMRS

Eidesstattliche Versicherung

Burian, Egon

Name, Vorname

Ich erkläre hiermit an Eides statt, dass ich die vorliegende Dissertation mit dem Titel:

Einsatz der Magnetresonanztomographie für die Detektion periapikaler Entzündungsprozesse und assoziierter mukosaler Pathologien

selbständig verfasst, mich außer der angegebenen keiner weiteren Hilfsmittel bedient und alle Erkenntnisse, die aus dem Schrifttum ganz oder annähernd übernommen sind, als solche kenntlich gemacht und nach ihrer Herkunft unter Bezeichnung der Fundstelle einzeln nachgewiesen habe.

Ich erkläre des Weiteren, dass die hier vorgelegte Dissertation nicht in gleicher oder in ähnlicher Form bei einer anderen Stelle zur Erlangung eines akademischen Grades eingereicht wurde.

München, 15.01.2024
Ort, Datum

Egon Burian
Unterschrift Doktorand

INHALTSVERZEICHNIS

1. ABKÜRZUNGSVERZEICHNIS

CT	Computertomographie
DVT	Digitale Volumentomographie
FOV	Field of View
MRT	Magnetresonanztomographie
OPT	Orthopanthomographie
PAI	Periapikalindex
STIR	Short tau inversion recovery
TR	Repetitionszeit
TE	Echozeit
ΔTE	Differenz der Echozeiten
UTE	Ultrashort echo time
ZTE	Zero echo time

2. EINLEITUNG & HINTERGRUND

2.1. Bildgebung in der Zahnmedizin

In der bildgebenden Diagnostik der Zahnmedizin nehmen projektionsradiographische Verfahren weiterhin einen großen Stellenwert ein, vor allem in den Subspezialisierungen der konservierenden Zahnmedizin wie der Endodontologie und der Parodontologie [1,2]. Sei es die Bissflügelaufnahme für die Detektion der Approximalkaries, das apikale Röntgen für die Darstellung apikaler Osteolysen oder die Orthopanthomographie (OPT) für die Einschätzung des Attachmentverlusts bei der generalisierten Parodontitis: viele Diagnosen und daraus abgeleitete Therapien basieren auf den Befunden der Projektionsradiographie [3-7].

Diese Techniken erlauben eine exzellente Detektion von Demineralisierungsprozessen, welche in Form von Radiotransluzenzen abgebildet werden und auf einer erleichterten Durchdringung der Hartgewebe durch ionisierende Röntgenstrahlen beruhen. Auf diesem Weg können sowohl mit einer hohen Sensitivität kariöse Läsion der Zahnhartsubstanz als auch apikalen Osteolysen bei einer vorliegenden apikalen Parodontitis detektiert werden [8-12]. Hier geht das Vorliegen der jeweiligen Pathologie mit der daraus resultierenden Therapie Hand in Hand. Im ersten Fall würde die Diagnose einer Karies eine Exkavation nach sich ziehen und im anderen Fall hätte die klinisch bestätigte irreversible Pulpitis mit assoziierter apikaler Osteolyse die Initiierung einer endodontischen Behandlung zur Folge. Die Problematik der niedrigen Sensitivität und des niedrigen negativen prädiktiven Wertes der OPT zur Detektion apikaler Osteolysen wurde bereits gezeigt, sodass weiterhin die Digitale Volumentomographie (DVT) der klinische Goldstandard bleibt [12].

Darüber hinaus wird die DVT sowohl zur präoperativen Planung vor Wurzelspitzenresektionen und Implantatinsertionen bei Fällen mit komplexer Anatomie eingesetzt als auch zur Evaluation des dreidimensionalen Attachmentverlustes bei aggressiven Formen der Parodontitis mit ausgedehntem vertikalen Knochendefekten [13-16]. Bei Vorliegen einer exazerbierten Entzündung oder Abszedierungen mit mutmaßlich dentogenem Ursprung kann die Durchführung einer Computertomographie (CT) sinnvoll sein, um die Affektion der Nachbarstrukturen besser beurteilen zu können. Besonders im Fall einer apikalen Osteolyse im Prämolaren- oder Molarenbereich des Oberkiefers kann dies erforderlich sein, um eine dentogene Sinusitis auszuschließen und eine aszendierende Abszedierung zu vermeiden [17-19].

Sowohl die bildgebenden Modalitäten der Projektionsradiographie als auch der Schnittbildgebung basieren auf der Durchdringung von Hart- und Weichgeweben durch ionisierende Röntgenstrahlen. Demineralisierungsprozesse dentogener oder ossärer Strukturen können unter Verwendung dieser Modalitäten mit einer hohen Spezifität im Falle der dentalen Radiographie und exzellenter räumlicher Auflösung bei der Verwendung der CT oder DVT dargestellt werden [12,20]. Darüber hinaus sind die flächendeckende Verfügbarkeit und die schnelle Durchführung der jeweiligen Bildgebung Vorteile dieser Methoden.

Es ist jedoch bereits durch in vitro und in vivo Studien bekannt, dass vor dem Verlust der Zahn- und Knochenhartsubstanz einige molekularbiologische Prozesse ablaufen, die mit der Einleitung einer Entzündungsmediatorkaskade und der zellulären Infiltration der jeweiligen Gewebe mit Monozyten, Leukozyten und Lymphozyten einhergeht [21-24]. Die Veränderung der osmotischen Gradienten führt darüber hinaus zur Extravasation von Wasser und Induktion einer Ödemformation [23]. Dieser Zusammenhang ist aus vielen Bereichen der skelettalen Bildgebung bekannt und wird durch den Einsatz von fettunterdrückten, wasser-gewichteten Sequenzen in der Magnetresonanztomographie (MRT) darstellbar gemacht, um initiale Entzündungsvorgänge zu visualisieren [25,26].

2.2. Magnetresonanztomographie in der Zahnmedizin

Die MRT wird in der Zahnmedizin unter allen Bildgebungsmodalitäten am seltensten eingesetzt. Eine der häufigsten Indikationen für die Durchführung einer MRT ist die Frage nach arthrogenen Veränderungen des Kiefergelenks, welche u.a. im Rahmen der Craniomandibulären Dysfunktion auftreten können. Unter Einsatz von örtlich und zeitlich aufgelösten Sequenzen können sowohl artikuläre als auch diskogene Pathologien in Ruhe und in Bewegung dargestellt werden [27-29].

In den letzten Jahren sind zunehmend Studien zum Einsatz der MRT bei der kieferorthopädischen und implantologischen Plaung aber auch zur Beurteilung des parodontalen Attachments erschienen, die das Indikationsspektrum der Modalität erweitern [30-33]. Neben der bereits bekannten verbesserten Darstellung von Weichgeweben ist durch diese Studien zunehmend die Visualisierung der knöchernen Strukturen des Alveolarkamms in den Vordergrund gerückt. Unter Verwendung spezieller Sequenzen mit sehr kurzen Echozeiten

wie der T1 gradient echo (GRE), der Ultrashort echo time (UTE) oder der Zero echo time (ZTE) Sequenz konnten in mehreren Studien eine dimensionsstabile Darstellung des Knochenabbaus bei der generalisierten Parodontitis aber auch eine genaue Abbildung eines Furkationsbefalls oder der Ausdehnung von Knochennekrosen gezeigt werden [32,34-36]. Die T1 GRE Sequenz weist im Vergleich zum Goldstandard DVT eine hohe Dimensionstreue auf und ist ähnlich verlässlich wie die CT bei der Frakturdetektion [37,38].

Neben den beschriebenen Anwendungsfeldern, bei denen vor allem eine dem CT bzw. DVT vergleichbare Auflösung der ossären Architektur im Vordergrund steht, sind vor allem Fragestellungen für den Einsatz der MRT interessant, die auf die Visualisierung von Veränderungen abzielen, die sowohl die projektionsradiographischen Modalitäten als auch die Schnittbildgebung an ihre Grenzen bringen. In der Radiologie des Achsenskeletts ist der Einsatz der MRT bei Fragestellungen üblich, die die Beurteilung des Ausmaßes einer Entzündung von knöchernen Strukturen erfordern [39]. Beispiele sind chronische Entzündungen bei Psoriasis-Arthritis, die Beurteilung einer Sakroiliitis bei Morbus Bechterew aber auch akute Erkrankungen wie die Spondylodiszitis [40].

Vor diesem Hintergrund wäre zunächst die Untersuchung einer möglichen Ausdehnung des Indikationsspektrums der MRT bei periapikalen Läsionen sinnvoll, die kein Korrelat in der Radiographie oder Schnittbildgebung haben. Die könnten möglicherweise in Form von Hyperintensitäten in T2-basierten, wasser-gewichteten Sequenzen wie der Short tau inversion recovery (STIR) Sequenz dargestellt werden, noch bevor eine periapikale Osteolyse auftritt. Dieser Zusammenhang konnte bereits bei der Bildgebung der generalisierten Parodontitis gezeigt werden [32]. Dadurch könnte ein weiterer Schritt in Richtung Früherkennung von subtilen dentogenen Pathologien gemacht werden und darüber hinaus die Exazerbation zu einer periapikalen, radikulären Zyste oder einer dentogenen Sinusitis verhindert werden.

Die Schwierigkeit liegt in diesem Kontext jedoch darin, die Entscheidung zu treffen, wann der Einsatz einer MRT indiziert ist und ob der Einsatz als Erstliniendiagnostik, wie es aktuell bei der OPT der Fall ist, Sinn macht. Hierzu sind zuvorderst Machbarkeitsstudien notwendig, um Tendenzen aufzuzeigen, die weitere multizentrische, prospektive Studien rechtfertigen.

2.3. Ziele des Promotionsprojektes

Vor diesem Hintergrund ist die Bearbeitung einer Vielzahl an Fragestellungen denkbar. Im Rahmen dieses Promotionsprojektes sollen durch die zwei vorgelegten Studien die

periapikalen Veränderungen in der MRT mit den konventionellen, projektionsradiographischen Modalitäten verglichen werden. Die durchgeführte MRT beinhaltet eine wasser-sensitive Sequenz, die STIR Sequenz, mittels derer die initialen, ödematösen Veränderungen der periapikalen Knochenmatrix visualisiert werden. Darüber hinaus wird eine Sequenz mit hoher Auflösung der ossären Strukturen (T1 GRE) durchgeführt.

In der ersten Arbeit wurden gesunde und endodontisch behandelte Zähne hinsichtlich persistierender periapikaler Veränderungen untersucht, um chronische, posttherapeutische Signalalterationen darzustellen. Zum Themenkomplex postendodontische Veränderungen ist im Rahmen einer Publikation von Kruse bereits bei 149 Patienten gezeigt worden, dass allein auf Basis der DVT nicht zwischen fibrotischem Narbengewebe und akuter Entzündung unterschieden werden kann [41].

In der zweiten Arbeit wurde die Assoziation von periapikalen Läsionen der Prämolaren und Molaren des Oberkiefers mit dem Auftreten einer basalen Schleimhautschwellung der Kieferhöhle untersucht. Im Rahmen der zahnärztlichen Initialuntersuchung inklusive einer Bildgebung durch OPT und/oder entsprechende Zahnfilme ist bei asymptomatischen Patienten die Detektion dentogener Sinusitiden erschwert. Diese können jedoch im Falle einer schleichenden Progredienz zu schwerwiegenden Komplikationen führen. Im Sinne einer Primärprävention wäre die Identifikation von symptomfreien Patienten mit bereits detektierbaren Veränderungen der Kieferhöhlenschleimhaut mittels MRT und der Vergleich mit den üblichen Verfahren interessant.

2.4. Eigenanteil

Ich war grundlegend bei der Ideenentstehung zum Einsatz der MRT in der Parodontologie beteiligt. Hier habe ich entscheidend bei der Konzeptualisierung der prospektiven Studie mitgewirkt, die initial auf die Detektion von frühen Veränderungen der Zahnhalteapparats im Rahmen einer Parodontitis ausgelegt war und bereits hochranging publiziert wurde. Darüber hinaus habe ich für das konzipierte Studiendesign den Ethikantrag verfasst. Auf der Grundlage dieses Ethikantrages entstanden bereits fünf Originalarbeiten. Bei der Entstehung des Scanprotokolls und der Etablierung der jeweiligen Sequenzen für den Themenkomplex Parodontologie und Mund-, Kiefer-, Gesichtschirurgie inklusive Nervbildgebung war ich neben Priv.-Doz. Dr. Monika Probst und Prof. Dr. Karampinos maßgeblich beteiligt. Hinzukommend war ich für die Analyse und klinische Befundung der MRT-Untersuchungen. Die Projektideen zu beiden Arbeiten des Promotionsprojektes entstanden in mehreren fachlichen Diskussionen

mit Prof. Dr. Dr. Matthias Folwaczny. Im Folgenden werden die jeweils konkreten Eigenanteile thematisiert.

2.4.1. Eigenanteil an Publikation I

An der vorgestellten Publikation 1 mit dem Titel „Evaluation of 3D MRI for early detection of bone edema associated with periapical lesions“, erschienen 2023 in Clinical Oral Investigations, war ich als Ko-Erstautor für folgende Punkte verantwortlich:

Projektdesign, Konzeptualisierung, Material und Methodik, Validierung, Datenerhebung, Dateninterpretation, Entwurf und Verfassen des Manuskripts, Revision des Manuskripts, Supervision, Projektadministration.

Da sich Herr Feuerriegel bei der Etablierung der dentalen Bildgebung im Institut für Radiologie zunehmend eingebracht hat sowie maßgeblich bei der Entstehung des Manuskriptes mitgewirkt hat, entschieden sich die Autoren für eine geteilte Erstautorenschaft um diesem Einsatz entsprechend Rechnung zu tragen.

2.4.2. Eigenanteil an Publikation II

An der vorgestellten Publikation 2 mit dem Titel „Visualization of clinically silent, odontogenic maxillary sinus mucositis originating from periapical inflammation using MRI: a feasibility study“, erschienen 2023 in Clinical Oral Investigations, war ich als Erstautor für folgende Punkte verantwortlich:

Projektdesign, Konzeptualisierung, Material und Methodik, Validierung, Datenerhebung, Dateninterpretation, Entwurf und Verfassen des Manuskripts, Revision des Manuskripts, Supervision, Projektadministration.

3. VORSTELLUNG DER ARBEITEN

3.1. Detektion von periapikalen Läsionen bei asymptomatischen und endodontisch vorbehandelten Zähnen

Feuerriegel GC*, Burian E*, Sollmann N, Leonhardt Y, Burian G, Griesbauer M, Bumm C, Makowski MR, Probst M, Karampinos DC, Folwaczny M.
*geteilte Erstautorenschaft

Hintergrund

Die apikale Parodontitis ist ein entzündlicher Prozess im Bereich der Wurzelspitze, der durch Pathogene und deren produzierte Toxine verursacht wird. Diese gelangen über das Wurzelkanalsystem bei Vorliegen einer Pulpitis oder über den Parodontalspalt nach periapikal [42]. Die komplexe Wechselwirkung von Mediatoren, mikrobiellen Antigenen und Toxinen führt schließlich zur periradikulären Entzündungsreaktion. Diese wiederum führt initial zu einer Veränderung osmotischer Gradienten über eine zunehmende Vasodilatation und im weiteren Verlauf zu einer lokalen Knochenresorption, welche in Form einer periapikalen Radiotransluzenz durch den Zahnfilm detektiert werden kann [4,43]. Die MRT bietet hier die Möglichkeit durch den Einsatz wasser-gewichteter Sequenzen den initialen Entzündungsprozess abzubilden. Das Potential der MRT für die Darstellung der parodontalen Entzündung noch vor dem irreversiblen Attachmentverlust konnte bereits durch unsere Arbeitsgruppe gezeigt werden [32].
Vor dem Hintergrund dieser Entwicklungen wurde in der durchgeführten Studie der Einsatz der MRT zur Detektion asymptomatischer, periapikaler Entzündungen in Form eines umschriebenen Knochenödems untersucht. Das Ziel der Studie war es, Korrelate periapikaler Läsionen im Alveolarknochen mittels 3T MRT zu detektieren und mit den korrespondierenden Veränderungen der OPT und Zahnröntgenaufnahmen zu vergleichen. Das übergeordnete Ziel der Studie war es, das Potenzial der MRT zur Früherkennung initialer entzündlicher Prozesse der Wurzelspitzen zu evaluieren.

Material und Methoden

In dieser Studie wurden 37 Patienten und 237 Zähne eingeschlossen (Alter: 62 ± 13.9 Jahre, davon 18 Frauen und 19 Männer). Alle Patienten wurden klinisch untersucht und erhielten ein OPT sowie eine 3T-MRT des Viszerokraniums. Die MR-Sequenzen wurden auf das Auftreten und Ausmaß von Knochenveränderungen im Zusammenhang mit periapikalen Läsionen

untersucht, darunter: Knochenödeme, periradikuläre Zysten und Granulome. OPTs und Zahnröntgenbilder, falls vorhanden, wurden anhand des Periapikalindex (PAI) auf entsprechende periapikale Aufhellungen untersucht und quantifiziert. Ein Radiologe sowie ein Radiologe und Zahnarzt befundeten die Bilder separat, unabhängig und in zufälliger Reihenfolge. Die Übereinstimmung zwischen den Modalitäten wurde mit dem Wilcoxon-Vorzeichen-Rang-Test bewertet. Die Inter- und Intrareader-Übereinstimmung wurde mit gewichtetem Cohens κ untersucht.

Ergebnisse

Von den 232 untersuchten Zähnen wiesen 69 ein reaktives Knochenödem mit entsprechender Radiotransluzenz im OPT auf. In 105 Fällen wurde im MRT ein Ödem ohne korrespondierende Aufhellung im OPT festgestellt. Aufhellungen im OPT ohne korrespondierendes Knochenödem im MRT wurden nicht gefunden. Die im MRT gemessene Ausdehnung des Ödems war signifikant größer als die Aufhellung im OPT (STIR-Mittelwert 2,4 mm ± 1,4 mm, Zahnröntgenbild-Mittelwert 1,3 mm ± 1,2 mm, OPT-Mittelwert 0,8 mm ± 1,1 mm, p = 0,01). Der PAI-Wert war im MRT ebenfalls signifikant größer als im konventionellen OPT (STIR mittlerer PAI 1,9 ± 0,7, Zahnröntgenbild mittlerer PAI 1,3 ± 0,5, OPT mittlerer PAI 1,2 ± 0,7, p = 0,02). Die *intra- und interreader* Übereinstimmung war sehr gut (Bereich κ 0,92–0,98 (95 % Konfidenzintervall 0,96–0,99), ICC 0,86–0,95 (95 % Konfidenzintervall 0,83–0,98)).

Schlussfolgerung

Durch die Verwendung flüssigkeitssensitiver MRT-Sequenzen wie der 3D STIR können periapikale Ödemformationen visualisiert werden, die einer Knochenresorbtion vorausgehen. Auf diese Weise können in frühen Entzündungsstadien wertvolle diagnostische Zusatzinformationen gewonnen werden, bevor diese in OPT und Zahnröntgen detektierbar sind. Aufgrund der überschaubaren Scanzeit von ca. 6 Minuten wäre ein Einsatz der MRT zur Detektion periapikaler Läsionen als komplementäre diagnostische Option zu den konventionellen Modalitäten denkbar.

3.2. Assoziation von periapikalen Veränderungen mit Schleimhautschwellungen in der Kieferhöhle bei asymptomatischen Patienten

Burian E, Feuerriegel GC, Sollmann N, Burian G, Palla B, Griesbauer M, Bumm C, Probst M, Beer M, Folwaczny M.

Hintergrund

Der unmittelbare Zusammenhang zwischen chronischen und akuten periapikalen Entzündungsprozessen der Oberkieferseitenzähne und der odontogenen Sinusitis ist bekannt [44]. Die Diagnose der odontogenen Sinusitis basiert auf der klinischen Untersuchung des symptomatischen Patienten und der Identifikation eines zugrunde liegenden Fokus, welcher meist auf eine periapikale Entzündungsreaktion zurückzuführen ist. In der klinischen Praxis werden zur Identifikation periapikaler Osteolysen Bildgebungsmodalitäten aus der Projektionsradiographie und der Schnittbildgebung eingesetzt [18,45]. Es ist jedoch erwiesen, dass eine periapikale Osteolyse ein Spätstadium einer chronischen Entzündung darstellt, welcher häufig eine kariesinduzierte Pulpitis oder eine Endo-Perio-Läsion vorausgeht. Bevor es jedoch zu einer Knochenresorption kommt, wird durch Zytokine und andere Entzündungsmediatoren eine Kaskade in Gang gesetzt, die zu lokalen ödematösen Veränderungen führt [21,23,46,47]. Bereits diese initialen, akuten periapikalen Veränderungen können bei bestehender anatomischer Nähe zum Kieferhöhlenboden per continuitatem zu einer lokalen Mukositis und bei Persistieren des Entzündungsreizes zu einer odontogenen Sinusitis führen, die symptomlos ablaufen kann und durch blande Befunde sowohl in der DVT, CT und im Röntgen unentdeckt bleibt.

Das Ziel dieser Studie war es, die Assoziation apikaler Entzündungsprozesse der Oberkieferseitenzähne mit einer lokalen Mukositis des Kieferhöhlenbodens mittels MRT zu visualisieren und mit dem Goldstandard der klinischen Praxis (OPT und Zahnfilm) zu vergleichen.

Material und Methoden

In die durchgeführte Studie wurden 16 asymptomatische Patienten mit einer Schleimhautschwellung der Kieferhöhle aufgenommen, die mittels MRT detektiert wurde. Die periapikalen Strukturen der Oberkieferseitenzähne wurden unter Verwendung einer Short-Tau-Inversion-Recovery (STIR)-Sequenz bewertet. Falls bestehend wurden apikale Pathologien mittels OPT, Zahnfilm und MRT unter Verwendung des periapikalen Index-Scores (PAI) beurteilt.

Die Dicke der Kieferhöhlenschleimhaut wurde in Millimetern unter Verwendung der koronalen, axialen und sagittalen Reformationen der STIR- nach Gürhan et al. und Shanbhaget al. ermittelt und in drei Klassen unterteilt [48,49]: Klasse I: 2,1–5 mm; Klasse II: 5,1–10 mm; und Klasse III: > 10 mm. Hinzukommend wurde die Konfiguration der Schleimhaut als „flach" (horizontale Verdickung der Sinusbodenschleimhaut) oder „polypös" (kuppelförmige Verdickung der Sinusbodenschleimhaut) klassifiziert. Die Bildanalyse wurde von einem Radiologen (4 Jahren Berufserfahrung) sowie einem Zahnarzt und Radiologen (7 Jahre Radiologieerfahrung, 2 Jahre Oralchirurgieerfahrung) durchgeführt. Bei starken Artefakten durch metallische Restaurationen oder Bewegungsartefakte wurden entsprechende Zähne von der weiteren Analyse ausgeschlossen.
Vergleiche zwischen den Gruppen wurden mit Chi-Quadrat-Tests mit Yates-Korrektur durchgeführt. Die Signifikanz wurde auf $p < 0,05$ festgelegt.

Ergebnisse

Bei allen eingeschlossenen Patienten (n = 16), die eine klinisch inapparente Mukositis aufwiesen (n = 21), konnten periapikale Entzündungen mit der MRT visualisiert werden. Das Knochenödem- und PAI-Scores waren in der MRT signifikant größer als korrespondierende Radiotransluzenzen in der OPT oder im Zahnfilm ($p < 0,05$). Unter Verwendung der STIR-Sequenz wurde eine signifikante Assoziation eines PAI-Scores größer 1 und dem Vorhandensein einer Mukositis festgestellt ($p = 0,03$).
Acht der 16 eingeschlossenen Patienten wurden aufgrund der ermittelten Schleimhautschwellung der Klasse I zugeordnet, 4 Probanden wiesen eine Klasse II und 9 Probanden wiesen eine Verdickung kaudalen Kieferhöhlenschleimhaut von mehr als 10 mm (Klasse III) auf. Durch die OPT und unter Verwendung von Zahnfilmen konnten bei lediglich zwei Patienten, die der Klasse I zugewiesen wurden, ein projektionsradiographisches Korrelat detektiert werden. Die Hälfte der Fälle aus der Klasse II konnten durch eine der beiden strahlenbasierten Modalitäten ermittelt werden. In der Klasse III zeigte sich bei 8 von 9 Patienten eine entsprechende Veränderung am Kieferhöhlenboden, die mit einer Mukositis zu vereinbaren war.

Schlussfolgerung

In dieser Studie konnte gezeigt werden, dass periapikale Ödemformationen der Oberkieferseitenbezahnung durch die MRT visualisiert werden konnten und mit dem Vorhandensein einer Schleimhautverdickung am Kieferhöhlenboden assoziiert waren. Diese Veränderungen waren noch vor Entstehung einer lokalen Knochenresorption zu erkennen. Bemerkenswerterweise waren die pathologischen, periapikalen Befunde im MRT nicht mit der Ausprägung der Schleimhautschwellung assoziiert. Allerdings konnten subtile Veränderungen

der Kieferhöhlenmukosa in früheren Stadien visualisiert werden als mittels konventioneller, projektionsradiographischer Methoden (OPT und Zahnfilm). Somit könnte die MRT zur Früherkennung von periapikalen Veränderungen mit assoziierter Schleimhautschwellung als mögliche komplementäre Bildgebung dienen. Die Möglichkeit zur Früherkennung dieser Pathologien könnte in Zukunft Einfluss auf diagnostische Kriterien und Therapieprotokolle haben.

4. ZUSAMMENFASSUNG

Die Diagnose der apikalen Parodontitis basiert auf dem Zusammenführen der Informationen, die aus der Anamnese, der klinischen Untersuchung und der Bildgebung gewonnen werden. Die strahlenbasierten Verfahren der Projektionsradiographie und der Schnittbildgebung bilden die Grundlage der zahnärztlichen Bildgebung. Das zahnärztliche Röntgen, die Orthopantomographie (OPT), die digitale Volumentomographie (DVT) und die Computertomographie (CT) erlauben es, ossäre und dentale Hartgebewebe mit einer hohen Auflösung darzustellen und ossäre Pathologien, wie Resorptionen und kariöse Läsionen, zu detektieren. Der Manifestation einer periapikalen Osteolyse bei Vorliegen einer Pulpitits gehen einige komplexe pathophysiologische Vorgänge voraus, die auf der Induktion einer Mediator- und Zytokinkaskade beruhen und mit einer lokalen Ödemformation einhergehen. In diesem Kontext ermöglicht die Magnetresonanztomographie (MRT) mit wasser-sensitiven Sequenzen die Visualisierung von lokalen Knochenödemen, die oftmals noch keine periapikalen Radiotransluzenzen aufweisen. In der klinischen Radiologie macht man sich diese Eigenschaft bestimmter MRT-Sequenzen zu Nutze, um bei chronischen Krankheiten wie der rheumatoiden Arthritis oder akuten Pathologien wie der Osteomyelitis pathologische Veränderungen des Knochenmarks zu erkennen und Verdachtsdiagnosen zu bestätigen.

Unter bestimmten Voraussetzungen können auch klinisch asymptomatische Zähne einen Fokus für diffuse Infektionen des Alveolarknochens und der umgebenden Weichgewebe darstellen. Insbesondere immunologisch kompromittierte oder onkologische Patienten gehören zu den Risikogruppen. Die Früherkennung von dentogenen Foci spielt vor allem bei der Prävention der Medikamenten-assoziierten Osteonekrose eine große Rolle. In diesem Kontext ist auch der odontogenen Sinusitis eine besondere Bedeutung beizumessen. Die Diagnose einer odontogenen Sinusitis wird im Falle eines klinischen Verdachts aus der Kombination aus klinischer Untersuchung und Befunden der OPT und CT gestellt.

Die im Rahmen dieser Doktorarbeit durchgeführten Studien evaluieren die Verwendung wasser-gewichteter MRT-Sequenzen (i) zur Visualisierung periapikaler Entzündungen und (ii) zur Detektion einer klinisch asymptomatischen Schleimhautschwellung des Oberkiefers, die mit einer periapikalen Entzündungen der oberen Prämolaren und Molaren assoziiert ist. In beiden Projekten wurde die MRT mit der konventionellen Bildgebung, bestehend aus der OPT und Zahnröntgenaufnahmen, verglichen.

Die Ergebnisse des ersten Projekts zeigen, dass die Visualisierung von periapikalen Ödemformationen als Korrelat für eine asymptomatische Entzündungsreaktion mittels MRT möglich war – und dies noch vor Manifestation einer Knochenresorption. In der zweiten Studie konnte gezeigt werden, dass periapikale Knochenödeme im Bereich der Oberkiefermolaren und Prämolaren, die im MRT erkannt wurden, mit dem Vorliegen einer Schleimhautverdickung am Kieferhöhlenboden assoziiert waren. Auch hier konnten umschriebene Ödeme, die im MRT detektiert wurden, vor Beginn der Knochenresorption abgegrenzt werden. Das Ausmaß des periapikalen Ödems im MRT war jedoch nicht mit dem Ausmaß der Entzündungsreaktion der Kieferhöhlenschleimhaut assoziiert.

Zusammenzufassend konnte durch die beiden durchgeführten Studien gezeigt werden, dass die Verwendung wasser-sensitiver MRT-Sequenzen die Früherkennung von periapikalen Knochenödemen ermöglicht, die als Korrelat für sowohl akute als auch chronische Entzündungsreaktionen gewertet werden können. Ödematöse Veränderungen, die mit der MRT visualisiert werden, können detektiert werden bevor eine ossäre Resorption in der Zahnröntgenaufnahme oder OPT abgrenzbar ist. Ein weiterer interessanter Aspekt der MR-Bildgebung ist die Möglichkeit der frühen Detektion sich auf Nachbargewebe ausbreitender Entzündungen. Beide Arbeiten, die im Rahmen der vorliegenden Dissertation durchführt wurden, unterstreichen das Potential der MRT im Bereich der konservierenden Zahnheilkunde im Sinne der Prävention und der Früherkennung von initialen Pathologien.

5. ABSTRACT

The diagnosis of apical periodontitis involves gathering patient history, conducting a clinical examination, and utilizing imaging techniques for further evaluation. In daily clinical practice, imaging techniques such as dental radiography, oral panoramic radiography (OPT) or cone beam computed tomography (CBCT) can display apical bone resorption. However, before osteoclast activity is upregulated and physiological bone turnover is disrupted, inflammatory cytokines released and toxin secretion induce edema formation by vasodilation. In contrast to conventional ionizing radiation-based techniques Magnetic Resonance Imaging (MRI) using water-sensitive sequences allow for bone edema imaging and thereby enable the clinician to detect subtle, localized inflammatory reactions. The concept of bone edema detection using MRI is well established in clinical imaging and has been used to detect changes in chronic diseases like rheumatoid arthritis or acute pathologies like osteomyelitis.

Even clinically asymptomatic teeth can cause diffuse infection of the alveolar bone and the maxillary mucosa. Especially in immunologically compromised or oncological patients who underwent irradiation or chemotherapy, early detection of periapical pathologies is of high relevance to avoid inflammation exacerbation. The early detection of odontogenic foci plays a major role in the prevention of radiation- or medication-induced osteonecrosis of the jaw. In this context, the presence of maxillary mucositis is clinically of high relevance, which is detected by OPT and verified by Computed Tomography (CT) if patients appear to have characteristic symptoms.

The studies conducted in context of this doctoral thesis evaluate the use of water-weighed MRI sequences (i) for the visualization of periapical inflammation and (ii) for the detection of clinically asymptomatic maxillary mucositis in association with periapical inflammation of the upper premolars and molars. In both projects MRI was compared to conventional dental imaging consisting of OPT and dental radiographs.

The results of the first project show that the visualization of periapical bone edema using MRI was feasible before bone resorption was detectable by dental radiography. Based on these results, we aimed to investigate on the association of periapical edema and inflammatory changes of the maxillary mucosa within a following study. Again, circumscribed edema detected by MRI could be delineated prior to the onset of bone resorption. However, the extent

of periapical edema in MRI was not associated with the severity of inflammatory reaction of the maxillary mucosa.

To sum up the two studies of this thesis, we show that early detection and assessment of periapical bone edema was feasible and accurate using water-sensitive MRI sequences. Edematous changes visualized with MRI were detectable before osteolysis was delineated in dental radiography or OPT. The second project verified that MRI can reveal an association of periapical edema and maxillary mucositis even in asymptomatic patients, emphasizing the potential of dedicated MRI sequences in preventive medicine and early disease detection.

6. LITERATURVERZEICHNIS

1. Patel S, Durack C, Abella F, Shemesh H, Roig M, Lemberg K. Cone beam computed tomography in Endodontics - a review. Int Endod J 2015;48:3-15.

2. Acar B, Kamburoglu K. Use of cone beam computed tomography in periodontology. World J Radiol 2014;6:139-47.

3. Shahbazian M, Vandewoude C, Wyatt J, Jacobs R. Comparative assessment of periapical radiography and CBCT imaging for radiodiagnostics in the posterior maxilla. Odontology 2015;103:97-104.

4. Cotti E, Schirru E. Present status and future directions: Imaging techniques for the detection of periapical lesions. Int Endod J 2022;55 Suppl 4:1085-99.

5. Papapanou PN, Sanz M, Buduneli N, et al. Periodontitis: Consensus report of workgroup 2 of the 2017 World Workshop on the Classification of Periodontal and Peri-Implant Diseases and Conditions. J Periodontol 2018;89 Suppl 1:S173-S82.

6. Persson RE, Tzannetou S, Feloutzis AG, Bragger U, Persson GR, Lang NP. Comparison between panoramic and intra-oral radiographs for the assessment of alveolar bone levels in a periodontal maintenance population. J Clin Periodontol 2003;30:833-9.

7. Grondahl HG, Jonsson E, Lindahl B. Diagnosis of periapical osteolytic processes with orthopantomography and intraoral full mouth radiography--a comparison. Sven Tandlak Tidskr 1970;63:679-86.

8. Obuchowicz R, Nurzynska K, Obuchowicz B, Urbanik A, Piorkowski A. Caries detection enhancement using texture feature maps of intraoral radiographs. Oral Radiol 2020;36:275-87.

9. Ekstrand KR, Ricketts DN, Kidd EA. Occlusal caries: pathology, diagnosis and logical management. Dent Update 2001;28:380-7.

10. Molander B, Ahlqwist M, Grondahl HG, Hollender L. Comparison of panoramic and intraoral radiography for the diagnosis of caries and periapical pathology. Dentomaxillofac Radiol 1993;22:28-32.

11. Petersson A, Axelsson S, Davidson T, et al. Radiological diagnosis of periapical bone tissue lesions in endodontics: a systematic review. Int Endod J 2012;45:783-801.

12. Nardi C, Calistri L, Grazzini G, et al. Is Panoramic Radiography an Accurate Imaging Technique for the Detection of Endodontically Treated Asymptomatic Apical Periodontitis? J Endod 2018;44:1500-8.

13. Assiri H, Dawasaz AA, Alahmari A, Asiri Z. Cone beam computed tomography (CBCT) in periodontal diseases: a Systematic review based on the efficacy model. BMC Oral Health 2020;20:191.

14. Mohan R, Mark R, Sing I, Jain A. Diagnostic Accuracy of CBCT for Aggressive Periodontitis. J Clin Imaging Sci 2014;4:2.

15. Rios HF, Borgnakke WS, Benavides E. The Use of Cone-Beam Computed Tomography in Management of Patients Requiring Dental Implants: An American Academy of Periodontology Best Evidence Review. J Periodontol 2017;88:946-59.

16. Kruse C, Spin-Neto R, Wenzel A, Kirkevang LL. Cone beam computed tomography and periapical lesions: a systematic review analysing studies on diagnostic efficacy by a hierarchical model. Int Endod J 2015;48:815-28.

17. Chong VF, Fan YF. Comparison of CT and MRI features in sinusitis. Eur J Radiol 1998;29:47-54.

18. Whyte A, Boeddinghaus R. Imaging of odontogenic sinusitis. Clinical radiology 2019;74:503-16.

19. Ghobrial GM, Pisculli ML, Evans JJ, Bilyk JR, Farrell CJ. Odontogenic Sinusitis Resulting in Abscess Formation Within the Optic Chiasm and Tract: Case Report and Review. J Neuroophthalmol 2016;36:393-8.

20. Leonardi Dutra K, Haas L, Porporatti AL, et al. Diagnostic Accuracy of Cone-beam Computed Tomography and Conventional Radiography on Apical Periodontitis: A Systematic Review and Meta-analysis. J Endod 2016;42:356-64.

21. Herrera BS, Martins-Porto R, Maia-Dantas A, et al. iNOS-derived nitric oxide stimulates osteoclast activity and alveolar bone loss in ligature-induced periodontitis in rats. J Periodontol 2011;82:1608-15.

22. Wan C, Yuan G, Yang J, et al. MMP9 deficiency increased the size of experimentally induced apical periodontitis. J Endod 2014;40:658-64.

23. Stashenko P, Teles R, D'Souza R. Periapical inflammatory responses and their modulation. Crit Rev Oral Biol Med 1998;9:498-521.

24. Silva MJ, Sousa LM, Lara VP, et al. The role of iNOS and PHOX in periapical bone resorption. J Dent Res 2011;90:495-500.

25. Miller TT, Randolph DA, Jr., Staron RB, Feldman F, Cushin S. Fat-suppressed MRI of musculoskeletal infection: fast T2-weighted techniques versus gadolinium-enhanced T1-weighted images. Skeletal Radiol 1997;26:654-8.

26. Sempere GA, Martinez Sanjuan V, Medina Chulia E, et al. MRI evaluation of inflammatory activity in Crohn's disease. AJR American journal of roentgenology 2005;184:1829-35.

27. Whyte AM, McNamara D, Rosenberg I, Whyte AW. Magnetic resonance imaging in the evaluation of temporomandibular joint disc displacement--a review of 144 cases. Int J Oral Maxillofac Surg 2006;35:696-703.

28. Bag AK, Gaddikeri S, Singhal A, et al. Imaging of the temporomandibular joint: An update. World J Radiol 2014;6:567-82.

29. Petscavage-Thomas JM, Walker EA. Unlocking the jaw: advanced imaging of the temporomandibular joint. AJR American journal of roentgenology 2014;203:1047-58.

30. Heil A, Lazo Gonzalez E, Hilgenfeld T, et al. Lateral cephalometric analysis for treatment planning in orthodontics based on MRI compared with radiographs: A feasibility study in children and adolescents. PLoS One 2017;12:e0174524.

31. Probst FA, Schweiger J, Stumbaum MJ, Karampinos D, Burian E, Probst M. Magnetic resonance imaging based computer-guided dental implant surgery-A clinical pilot study. Clin Implant Dent Relat Res 2020;22:612-21.

32. Probst M, Burian E, Robl T, et al. Magnetic resonance imaging as a diagnostic tool for periodontal disease: A prospective study with correlation to standard clinical findings-Is there added value? J Clin Periodontol 2021;48:929-48.

33. Newbould RD, Bishop CA, Janiczek RL, Parkinson C, Hughes FJ. T2 relaxation mapping MRI of healthy and inflamed gingival tissue. Dentomaxillofac Radiol 2017;46:20160295.

34. Juerchott A, Sohani M, Schwindling FS, et al. In vivo accuracy of dental magnetic resonance imaging in assessing maxillary molar furcation involvement: A feasibility study in humans. J Clin Periodontol 2020;47:809-15.

35. Juerchott A, Sohani M, Schwindling FS, et al. Comparison of non-contrast-enhanced dental magnetic resonance imaging and cone-beam computed tomography in assessing the horizontal and vertical components of furcation defects in maxillary molars: An in vivo feasibility study. J Clin Periodontol 2020;47:1485-95.

36. Schumann P, Morgenroth S, Huber FA, Rupp NJ, Del Grande F, Guggenberger R. Correlation of dynamic contrast-enhanced bone perfusion with morphologic ultra-short echo time MR imaging in medication-related osteonecrosis of the jaw. Dentomaxillofac Radiol 2022;51:20210036.

37. Probst FA, Burian E, Malenova Y, et al. Geometric accuracy of magnetic resonance imaging-derived virtual 3-dimensional bone surface models of the mandible in comparison to computed tomography and cone beam computed tomography: A porcine cadaver study. Clin Implant Dent Relat Res 2021;23:779-88.

38. Feuerriegel GC, Ritschl LM, Sollmann N, et al. Imaging of traumatic mandibular fractures in young adults using CT-like MRI: a feasibility study. Clin Oral Investig 2022.

39. Baraliakos X, Hermann KG, Landewe R, et al. Assessment of acute spinal inflammation in patients with ankylosing spondylitis by magnetic resonance imaging: a comparison between contrast enhanced T1 and short tau inversion recovery (STIR) sequences. Ann Rheum Dis 2005;64:1141-4.

40. Jimenez-Boj E, Nobauer-Huhmann I, Hanslik-Schnabel B, et al. Bone erosions and bone marrow edema as defined by magnetic resonance imaging reflect true bone marrow inflammation in rheumatoid arthritis. Arthritis Rheum 2007;56:1118-24.

41. Kruse C, Spin-Neto R, Reibel J, Wenzel A, Kirkevang LL. Diagnostic validity of periapical radiography and CBCT for assessing periapical lesions that persist after endodontic surgery. Dentomaxillofac Radiol 2017;46:20170210.

42. Tiburcio-Machado CS, Michelon C, Zanatta FB, Gomes MS, Marin JA, Bier CA. The global prevalence of apical periodontitis: a systematic review and meta-analysis. Int Endod J 2020.

43. Karamifar K, Tondari A, Saghiri MA. Endodontic Periapical Lesion: An Overview on the Etiology, Diagnosis and Current Treatment Modalities. Eur Endod J 2020;5:54-67.

44. Craig JR. Odontogenic sinusitis: A state-of-the-art review. World J Otorhinolaryngol Head Neck Surg 2022;8:8-15.

45. Shukairy MK, Burmeister C, Ko AB, Craig JR. Recognizing odontogenic sinusitis: A national survey of otolaryngology chief residents. Am J Otolaryngol 2020;41:102635.

46. Takahama A, Jr., Rocas IN, Faustino ISP, et al. Association between bacteria occurring in the apical canal system and expression of bone-resorbing mediators and matrix metalloproteinases in apical periodontitis. Int Endod J 2018;51:738-46.

47. Braz-Silva PH, Bergamini ML, Mardegan AP, De Rosa CS, Hasseus B, Jonasson P. Inflammatory profile of chronic apical periodontitis: a literature review. Acta Odontol Scand 2019;77:173-80.

48. Gurhan C, Sener E, Mert A, Sen GB. Evaluation of factors affecting the association between thickening of sinus mucosa and the presence of periapical lesions using cone beam CT. Int Endod J 2020;53:1339-47.

49. Shanbhag S, Karnik P, Shirke P, Shanbhag V. Association between periapical lesions and maxillary sinus mucosal thickening: a retrospective cone-beam computed tomographic study. J Endod 2013;39:853-7.

7. REFERENZLISTE EINGEBRACHTE ARBEITEN

7.1. Publikation I

Feuerriegel GC*, **Burian E*,** Sollmann N, Leonhardt Y, Burian G, Griesbauer M, Bumm C, Makowski RM, Probst M, Probst FA, Karampinos DC, Folwaczny M. Evaluation of 3D MRI for early detection of bone edema associated with periapical lesions. Clin Oral Investig 2023 Jul 18. doi: 10.1007/s00784-023-05159-z. Online ahead of print.

*Geteilte Erstautorenschaft

Die Ergebnisse der ersten Publikation wurden am 08.06.2023 auf der Jahrestagung der Schweizer Gesellschaft für Neuroradiologie vorgestellt. Hierfür wurde der Promovend mit dem ***Best Abstract Preis*** ausgezeichnet.
SGNR Annual Meeting 2023, 08.06-09.06.2023, Zürich
„Evaluation of 3D MRI for early detection of bone edema associated with periapical lesions"
Burian E, Feuerriegel GC, Probst M, Burian G, Folwaczny M, Sollmann N.

7.2. Publikation II

Burian E, Feuerriegel G, Sollmann N, Burian G, Palla B, Griesbauer M, Bumm C, Probst M, Beer M, Folwaczny M. Visualization of clinically silent, odontogenic maxillary sinus mucositis originating from periapical inflammation using MRI: a feasibility study. Clin Oral Investig. 2023 Apr 11. doi: 10.1007/s00784-023-04986-4. Online ahead of print.

8. CURRICULUM VITAE

9. PUBLIKATIONSVERZEICHNIS

Impact Faktor insgesamt: 270 (Erst-oder Letztautorenschaft: 75)
H-Faktor 17

*geteilte Erst-oder Letztautorenschaft

[1] S. Ziegelmayer, S. Reischl, H. Havrda, J. Gawlitza, M. Graf, N. Lenhart, N. Nehls, T. Lemke, D. Wilhelm, F. Lohofer, **E. Burian**, P.A. Neumann, M. Makowski, and R. Braren, Development and Validation of a Deep Learning Algorithm to Differentiate Colon Carcinoma From Acute Diverticulitis in Computed Tomography Images. JAMA Netw Open 6 (2023) e2253370. **IF 13,37**

[2] G.C. Feuerriegel, L.M. Ritschl, N. Sollmann, B. Palla, Y. Leonhardt, L. Maier, F.T. Gassert, D.C. Karampinos, M.R. Makowski, C. Zimmer, K.D. Wolff, M. Probst, A.M. Fichter*, and **E. Burian***, Imaging of traumatic mandibular fractures in young adults using CT-like MRI: a feasibility study. Clin Oral Investig 27 (2023) 1227-1233. **IF 3,6**

[3] **E. Burian***, D. Sepp*, M. Lehm, K. Bernkopf, S. Wunderlich, I. Riederer, C. Maegerlein, A. Alegiani, C. Zimmer, T. Boeckh-Behrens, and G.-E. Investigators, Start, Stop, Continue? The Benefit of Overlapping Intravenous Thrombolysis and Mechanical Thrombectomy : A Matched Case-control Analysis from the German Stroke Registry. Clin Neuroradiol 33 (2023) 187-197. **IF 3,1**

[4] **E. Burian*,** G. Feuerriegel, N. Sollmann, G. Burian, B. Palla, M. Griesbauer, C. Bumm, M. Probst, M. Beer, and M. Folwaczny, Visualization of clinically silent, odontogenic maxillary sinus mucositis originating from periapical inflammation using MRI: a feasibility study. Clin Oral Investig (2023). **IF 3,6**

[5] A. Barner, **E. Burian**, A. Simon, K. Castillo, B. Waschulzik, R. Braren, U. Heemann, J. Osterwalder, A. Spiel, M. Heim, and K.F. Stock, Pulmonary Findings in Hospitalized COVID-19 Patients Assessed by Lung Ultrasonography (LUS) - A Prospective Registry Study. Ultraschall Med (2023). **IF 4,6**

[6] Y. Leonhardt, M. Dieckmeyer, F. Zoffl, G.C. Feuerriegel, N. Sollmann, D. Junker, T. Greve, C. Holzapfel, H. Hauner, K. Subburaj, J.S. Kirschke, D.C. Karampinos, C. Zimmer, M.R. Makowski, T. Baum, and **E. Burian**, Associations of Texture Features of Proton Density Fat Fraction Maps between Lumbar Vertebral Bone Marrow and Paraspinal Musculature. Biomedicines 10 (2022). **IF 4,7**

[7] F.N. Harder, K. Weiss, T. Amiel, J.M. Peeters, R. Tauber, S. Ziegelmayer, **E. Burian**, M.R. Makowski, A.P. Sauter, J.E. Gschwend, D.C. Karampinos, and R.F. Braren, Prospectively Accelerated T2-Weighted Imaging of the Prostate by Combining Compressed SENSE and Deep Learning in Patients with Histologically Proven Prostate Cancer. Cancers (Basel) 14 (2022). **IF 6,5**

[8] T. Greve, N.M. Rayudu, M. Dieckmeyer, C. Boehm, S. Ruschke, **E. Burian**, C. Kloth, J.S. Kirschke, D.C. Karampinos, T. Baum, K. Subburaj, and N. Sollmann, Finite Element Analysis of Osteoporotic and Osteoblastic Vertebrae and Its Association With the Proton Density Fat Fraction From Chemical Shift Encoding-Based Water-Fat MRI - A Preliminary Study. Front Endocrinol (Lausanne) 13 (2022) 900356. **IF 6,0**

[9] **E. Burian**, B. Palla, N. Callahan, T. Pyka, C. Wolff, C.E. von Schacky, A. Schmid, M.F. Froelich, J. Rubenthaler, M.R. Makowski, and F.G. Gassert, Comparison of CT, MRI, and F-18 FDG PET/CT for initial N-staging of oral squamous cell carcinoma: a cost-effectiveness analysis. European journal of nuclear medicine and molecular imaging 49 (2022) 3870-3877. **IF 10,0**

[10] M. Dieckmeyer, S. Inhuber, S. Schlager, D. Weidlich, M.R.K. Mookiah, K. Subburaj, **E. Burian**, N. Sollmann, J.S. Kirschke, D.C. Karampinos, and T. Baum, Association of Thigh Muscle Strength with Texture Features Based on Proton Density Fat Fraction Maps Derived from Chemical Shift Encoding-Based Water-Fat MRI. Diagnostics (Basel) 11 (2021). **IF 3,9**

[11] M. Dieckmeyer, S. Inhuber, S. Schlaeger, D. Weidlich, M.R.K. Mookiah, K. Subburaj, **E. Burian**, N. Sollmann, J.S. Kirschke, D.C. Karampinos, and T. Baum, Texture Features of Proton Density Fat Fraction Maps from Chemical Shift Encoding-Based MRI Predict Paraspinal Muscle Strength. Diagnostics (Basel) 11 (2021). **IF 3,9**

[12] L. Patzelt, D. Junker, J. Syvari, **E. Burian**, M. Wu, O. Prokopchuk, U. Nitsche, M.R. Makowski, R.F. Braren, S. Herzig, M.B. Diaz, and D.C. Karampinos, MRI-Determined Psoas Muscle Fat Infiltration Correlates with Severity of Weight Loss during Cancer Cachexia. Cancers (Basel) 13 (2021). **IF 6,5**

[13] F.A. Probst, **E. Burian**, Y. Malenova, P. Lyutskanova, M.J. Stumbaum, L.M. Ritschl, S. Kronthaler, D. Karampinos, and M. Probst, Geometric accuracy of magnetic resonance imaging-derived virtual 3-dimensional bone surface models of the mandible in comparison to computed tomography and cone beam computed tomography: A porcine cadaver study. Clin Implant Dent Relat Res 23 (2021) 779-788. **IF 4,1**

[14] **E. Burian**, L. Grundl, T. Greve, D. Junker, N. Sollmann, M. Loffler, M.R. Makowski, C. Zimmer, J.S. Kirschke, and T. Baum, Local Bone Mineral Density, Subcutaneous and Visceral Adipose Tissue Measurements in Routine Multi Detector Computed Tomography-Which Parameter Predicts Incident Vertebral Fractures Best? Diagnostics (Basel) 11 (2021). **IF 3,9**

[15] N. Sollmann, E.A. Becherucci, C. Boehm, M.E. Husseini, S. Ruschke, **E. Burian**, J.S. Kirschke, T.M. Link, K. Subburaj, D.C. Karampinos, R. Krug, T. Baum, and M. Dieckmeyer, Texture Analysis Using CT and Chemical Shift Encoding-Based Water-Fat MRI Can Improve Differentiation Between Patients With and Without Osteoporotic Vertebral Fractures. Front Endocrinol (Lausanne) 12 (2021) 778537. **IF 6,0**

[16] M. Dieckmeyer, N.M. Rayudu, L.Y. Yeung, M. Loffler, A. Sekuboyina, **E. Burian**, N. Sollmann, J.S. Kirschke, T. Baum, and K. Subburaj, Prediction of incident vertebral fractures in routine MDCT: Comparison of global texture features, 3D finite element parameters and volumetric BMD. Eur J Radiol 141 (2021) 109827. **IF 4,5**

[17] M. Probst, **E. Burian**, T. Robl, D. Weidlich, D. Karampinos, T. Brunner, C. Zimmer, F.A. Probst, and M. Folwaczny, Magnetic resonance imaging as a diagnostic tool for periodontal disease: A prospective study with correlation to standard clinical findings-Is there added value? J Clin Periodontol 48 (2021) 929-948. **IF 7,4**

[18] L.Y. Yeung, N.M. Rayudu, M. Loffler, A. Sekuboyina, **E. Burian**, N. Sollmann, M. Dieckmeyer, T. Greve, J.S. Kirschke, K. Subburaj, and T. Baum, Prediction of Incidental Osteoporotic Fractures at Vertebral-Specific Level Using 3D Non-Linear Finite Element Parameters Derived from Routine Abdominal MDCT. Diagnostics (Basel) 11 (2021). **IF 3,9**

[19] N. Sollmann, N.M. Rayudu, L.Y. Yeung, A. Sekuboyina, **E. Burian**, M. Dieckmeyer, M.T. Loffler, B.J. Schwaiger, A.S. Gersing, J.S. Kirschke, T. Baum, and K. Subburaj, MDCT-Based Finite Element Analyses: Are Measurements at the Lumbar Spine Associated with the Biomechanical Strength of Functional Spinal Units of Incidental Osteoporotic Fractures along the Thoracolumbar Spine? Diagnostics (Basel) 11 (2021). **IF 3,9**

[20] N. Sollmann, N.M. Rayudu, J.J.S. Lim, M. Dieckmeyer, **E. Burian**, M.T. Loffler, J.S. Kirschke, T. Baum, and K. Subburaj, Multi-detector computed tomography (MDCT) imaging: association of bone texture parameters with finite element analysis (FEA)-based failure load of single vertebrae and functional spinal units. Quant Imaging Med Surg 11 (2021) 2955-2967. **IF 4,6**

[21] J. Schneider, H. Mijocevic, K. Ulm, B. Ulm, S. Weidlich, S. Wurstle, K. Rothe, M. Treiber, R. Iakoubov, U. Mayr, T. Lahmer, S. Rasch, A. Herner, **E. Burian**, F. Lohofer, R. Braren, M.R. Makowski, R.M. Schmid, U. Protzer, C. Spinner, and F. Geisler, SARS-CoV-2 serology increases diagnostic accuracy in CT-suspected, PCR-negative COVID-19 patients during pandemic. Respir Res 22 (2021) 119. **IF 7,1**

[22] B. Palla, **E. Burian**, A. Deek, C. Scott, J. Anderson, N. Callahan, and E.R. Carlson, Comparing the Surgical Response of Bisphosphonate-Related Versus Denosumab-Related Osteonecrosis of the Jaws. J Oral Maxillofac Surg 79 (2021) 1045-1052. **IF 2,1**

[23] S. Otto, S. Aljohani, R. Fliefel, S. Ecke, O. Ristow, **E. Burian**, M. Troeltzsch, C. Pautke, and M. Ehrenfeld, Infection as an Important Factor in Medication-Related Osteonecrosis of the Jaw (MRONJ). Medicina (Kaunas) 57 (2021). **IF 2,9**

[24] M.T. Loffler, A. Jacob, A. Scharr, N. Sollmann, **E. Burian**, M. El Husseini, A. Sekuboyina, G. Tetteh, C. Zimmer, J. Gempt, T. Baum, and J.S. Kirschke, Automatic opportunistic osteoporosis screening in routine CT: improved prediction of patients with prevalent vertebral fractures compared to DXA. European radiology 31 (2021) 6069-6077. **IF 7,0**

[25] F. Kofler, I. Ezhov, L. Fidon, C.M. Pirkl, J.C. Paetzold, **E. Burian**, S. Pati, M. El Husseini, F. Navarro, S. Shit, J. Kirschke, S. Bakas, C. Zimmer, B. Wiestler, and B.H. Menze, Robust, Primitive, and

Unsupervised Quality Estimation for Segmentation Ensembles. Front Neurosci 15 (2021) 752780. **IF 5,1**

[26] T. Greve, M. Sukopp, M. Wostrack, **E. Burian**, C. Zimmer, and B. Friedrich, Initial Raymond-Roy Occlusion Classification but not Packing Density Defines Risk for Recurrence after Aneurysm Coiling. Clin Neuroradiol 31 (2021) 391-399. **IF 3,1**

[27] T. Greve, **E. Burian**, A. Zoffl, G. Feuerriegel, S. Schlaeger, M. Dieckmeyer, N. Sollmann, E. Klupp, D. Weidlich, S. Inhuber, M. Loffler, F. Montagnese, M. Deschauer, B. Schoser, S. Bublitz, C. Zimmer, D.C. Karampinos, J.S. Kirschke, and T. Baum, Regional variation of thigh muscle fat infiltration in patients with neuromuscular diseases compared to healthy controls. Quant Imaging Med Surg 11 (2021) 2610-2621. **IF 4,6**

[28] J. Erber, J.R. Wiessner, G.S. Zimmermann, P. Barthel, **E. Burian**, F. Lohofer, E. Martens, H. Mijocevic, S. Rasch, R.M. Schmid, C.D. Spinner, R. Braren, J. Schneider, and T. Lahmer, Longitudinal Assessment of Health and Quality of Life of COVID-19 Patients Requiring Intensive Care-An Observational Study. J Clin Med 10 (2021). **IF 4,9**

[29] Q. Dou, T.Y. So, M. Jiang, Q. Liu, V. Vardhanabhuti, G. Kaissis, Z. Li, W. Si, H.H.C. Lee, K. Yu, Z. Feng, L. Dong, **E. Burian**, F. Jungmann, R. Braren, M. Makowski, B. Kainz, D. Rueckert, B. Glocker, S.C.H. Yu, and P.A. Heng, Federated deep learning for detecting COVID-19 lung abnormalities in CT: a privacy-preserving multinational validation study. NPJ Digit Med 4 (2021) 60. **IF 15,3**

[30] **E. Burian,** N. Sollmann, K. Mei, M. Dieckmeyer, D. Juncker, M. Loffler, T. Greve, C. Zimmer, J.S. Kirschke, T. Baum, and P.B. Noel, Low-dose MDCT: evaluation of the impact of systematic tube current reduction and sparse sampling on quantitative paraspinal muscle assessment. Quant Imaging Med Surg 11 (2021) 3042-3050. **IF 4,6**

[31] **E. Burian**, E.A. Becherucci, D. Junker, N. Sollmann, T. Greve, H. Hauner, C. Zimmer, J.S. Kirschke, D.C. Karampinos, K. Subburaj, T. Baum, and M. Dieckmeyer, Association of Cervical and Lumbar Paraspinal Muscle Composition Using Texture Analysis of MR-Based Proton Density Fat Fraction Maps. Diagnostics (Basel) 11 (2021). **IF 3,9**

[32] **E. Burian**, J. Syvari, M. Dieckmeyer, C. Holzapfel, T. Drabsch, N. Sollmann, J.S. Kirschke, E.J. Rummeny, C. Zimmer, H. Hauner, D.C. Karampinos, T. Baum, and D. Junker, Age- and BMI-related variations of fat distribution in sacral and lumbar bone marrow and their association with local muscle fat content. Sci Rep 10 (2020) 9686. **IF 4,9**

[33] **E. Burian,** D. Franz, T. Greve, M. Dieckmeyer, C. Holzapfel, T. Drabsch, N. Sollmann, M. Probst, J.S. Kirschke, E.J. Rummeny, C. Zimmer, H. Hauner, D.C. Karampinos, and T. Baum, Age- and gender-related variations of cervical muscle composition using chemical shift encoding-based water-fat MRI. Eur J Radiol 125 (2020) 108904. **IF 4,5**

[34] **E. Burian***, S. Inhuber*, S. Schlaeger, M. Dieckmeyer, E. Klupp, D. Franz, D. Weidlich, N. Sollmann, M. Loffler, A. Schwirtz, E.J. Rummeny, C. Zimmer, J.S. Kirschke, D.C. Karampinos, and T. Baum, Association of thigh and paraspinal muscle composition in young adults using chemical shift encoding-based water-fat MRI. Quant Imaging Med Surg 10 (2020) 128-136. **IF 4,6**

[35] N. Sollmann, A. Zoffl, D. Franz, J. Syvari, M. Dieckmeyer, **E. Burian**, E. Klupp, D.M. Hedderich, C. Holzapfel, T. Drabsch, J.S. Kirschke, E.J. Rummeny, C. Zimmer, H. Hauner, D.C. Karampinos, and T. Baum, Regional variation in paraspinal muscle composition using chemical shift encoding-based water-fat MRI. Quant Imaging Med Surg 10 (2020) 496-507. **IF 4,6**

[36] **E. Burian**, F.A. Probst, D. Weidlich, C.P. Cornelius, L. Maier, T. Robl, C. Zimmer, D.C. Karampinos, L.M. Ritschl, and M. Probst, MRI of the inferior alveolar nerve and lingual nerve-anatomical variation and morphometric benchmark values of nerve diameters in healthy subjects. Clin Oral Investig 24 (2020) 2625-2634. **IF 3,6**

[37] M.T. Loffler, N. Sollmann, **E. Burian,** A. Bayat, K. Aftahy, T. Baum, B. Meyer, Y.M. Ryang, and J.S. Kirschke, Opportunistic Osteoporosis Screening Reveals Low Bone Density in Patients With Screw Loosening After Lumbar Semi-Rigid Instrumentation: A Case-Control Study. Front Endocrinol (Lausanne) 11 (2020) 552719. **IF 6,0**

[38] N. Sollmann, D. Franz, **E. Burian,** M.T. Loffler, M. Probst, A. Gersing, B. Schwaiger, D. Pfeiffer, J.S. Kirschke, T. Baum, and I. Riederer, Assessment of paraspinal muscle characteristics, lumbar BMD, and their associations in routine multi-detector CT of patients with and without osteoporotic vertebral fractures. Eur J Radiol 125 (2020) 108867. **IF 4,5**

[39] F.A. Probst, J. Schweiger, M.J. Stumbaum, D. Karampinos, **E. Burian**, and M. Probst, Magnetic resonance imaging based computer-guided dental implant surgery-A clinical pilot study. Clin Implant Dent Relat Res 22 (2020) 612-621. **IF 4,1**

[40] N. Sollmann, M. Gutbrod-Fernandez, **E. Burian**, I. Riederer, B. Meyer, A. Hock, J. Gempt, C. Zimmer, and J.S. Kirschke, Subtraction Maps Derived from Longitudinal Magnetic Resonance Imaging in Patients with Glioma Facilitate Early Detection of Tumor Progression. Cancers (Basel) 12 (2020). **IF 6,5**

[41] F.A. Probst, R. Fliefel, **E. Burian**, M. Probst, M. Eddicks, M. Cornelsen, C. Riedl, H. Seitz, A. Aszodi, M. Schieker, and S. Otto, Bone regeneration of minipig mandibular defect by adipose derived mesenchymal stem cells seeded tri-calcium phosphate- poly(D,L-lactide-co-glycolide) scaffolds. Sci Rep 10 (2020) 2062. **IF 4,9**

[42] M. Dieckmeyer, F. Zoffl, L. Grundl, S. Inhuber, S. Schlaeger, **E. Burian**, C. Zimmer, J.S. Kirschke, D.C. Karampinos, T. Baum, and N. Sollmann, Association of quadriceps muscle, gluteal muscle, and femoral bone marrow composition using chemical shift encoding-based water-fat MRI: a preliminary study in healthy young volunteers. Eur Radiol Exp 4 (2020) 35.

[43] M. Dieckmeyer, D. Junker, S. Ruschke, M.R.K. Mookiah, K. Subburaj, **E. Burian**, N. Sollmann, J.S. Kirschke, D.C. Karampinos, and T. Baum, Vertebral Bone Marrow Heterogeneity Using Texture Analysis of Chemical Shift Encoding-Based MRI: Variations in Age, Sex, and Anatomical Location. Front Endocrinol (Lausanne) 11 (2020) 555931.

IF 6,0

[44] I. Cordts, M. Deschauer, P. Lingor, **E. Burian**, T. Baum, C. Zimmer, C. Maegerlein, and N. Sollmann, Radiation dose reduction for CT-guided intrathecal nusinersen administration in adult patients with spinal muscular atrophy. Sci Rep 10 (2020) 3406.

IF 4,9

[45] **E. Burian**, N. Sollmann, L.M. Ritschl, B. Palla, L. Maier, C. Zimmer, F. Probst, A. Fichter, M. Miloro, and M. Probst, High resolution MRI for quantitative assessment of inferior alveolar nerve impairment in course of mandible fractures: an imaging feasibility study. Sci Rep 10 (2020) 11566. **IF 4,9**

[46] **E. Burian***, F. Jungmann*, G.A. Kaissis*, F.K. Lohofer, C.D. Spinner, T. Lahmer, M. Treiber, M. Dommasch, G. Schneider, F. Geisler, W. Huber, U. Protzer, R.M. Schmid, M. Schwaiger, M.R. Makowski, and R.F. Braren, Intensive Care Risk Estimation in COVID-19 Pneumonia Based on Clinical and Imaging Parameters: Experiences from the Munich Cohort. J Clin Med 9 (2020). **IF 4,9**

[47] **E. Burian,** A. Rohrmeier, S. Schlaeger, M. Dieckmeyer, M.N. Diefenbach, J. Syvari, E. Klupp, D. Weidlich, C. Zimmer, E.J. Rummeny, D.C. Karampinos, J.S. Kirschke, and T. Baum, Lumbar muscle and vertebral bodies segmentation of chemical shift encoding-based water-fat MRI: the reference database MyoSegmenTUM spine. BMC Musculoskelet Disord 20 (2019) 152.

IF 2,5

[48] S. Inhuber, N. Sollmann, S. Schlaeger, M. Dieckmeyer, **E. Burian**, C. Kohlmeyer, D.C. Karampinos, J.S. Kirschke, T. Baum, F. Kreuzpointner, and A. Schwirtz, Associations of thigh muscle fat infiltration with isometric strength measurements based on chemical shift encoding-based water-fat magnetic resonance imaging. Eur Radiol Exp 3 (2019) 45.

[49] Burian E, Subburaj K, Mookiah MRK, Rohrmeier A, Hedderich DM, Dieckmeyer M, Diefenbach NM, Ruschke S, Rummeny EJ, Zimmer C, Kirschke JS, Karampinos DC, Baum T. Texture analysis of vertebral bone marrow using chemical shift encoding-based water-fat MRI: a feasibility study. Osteoporosis International. 2019 March; 30:1265–1274. doi: 10.1007/s00198-019-04924-9.

IF 5,1

[50] **E. Burian**, J. Syvari, C. Holzapfel, T. Drabsch, J.S. Kirschke, E.J. Rummeny, C. Zimmer, H. Hauner, D.C. Karampinos, T. Baum, and D. Franz, Gender- and Age-Related Changes in Trunk Muscle Composition Using Chemical Shift Encoding-Based Water(-)Fat MRI. Nutrients 10 (2018). **IF 5,7**

[51] M. Probst, S. Koerdt, L.M. Ritschl, O. Bissinger, F. Liesche, J. Gempt, B. Meyer, **E. Burian**, N. Lummel, and A. Kolk, Malignant Peripheral Nerve Sheath Tumor in the Course of the Mandibular Nerve. World Neurosurg 117 (2018) e130-e137. **IF 2,2**

[52] B. Palla, **E. Burian,** R. Fliefel, and S. Otto, Systematic review of oral manifestations related to hyperparathyroidism. Clin Oral Investig 22 (2018) 1-27. **IF 3,6**

[53] S. Otto, **E. Burian**, M. Troeltzsch, G. Kaeppler, and M. Ehrenfeld, Denosumab as a potential treatment alternative for patients suffering from diffuse sclerosing osteomyelitis of the mandible-A rapid communication. J Craniomaxillofac Surg 46 (2018) 534-537.

IF 3,1

[54] S. Otto, C. Kleye, **E. Burian**, M. Ehrenfeld, and C.P. Cornelius, Custom-milled individual allogeneic bone grafts for alveolar cleft osteoplasty-A technical note. J Craniomaxillofac Surg 45 (2017) 1955-1961. **IF 3,1**

[55] M. Cornelsen, F.A. Probst, C. Schwarz, **E. Burian,** M. Troltzsch, S. Otto, M.M. Saller, M. Schieker, and H. Seitz, Mechanical and biological effects of infiltration with biopolymers on 3D printed tricalciumphosphate scaffolds. Dent Mater J 36 (2017) 553-559. **IF 3,4**

[56] **E. Burian**, C. Schulz, F. Probst, B. Palla, M. Troltzsch, F. Maglitto, L. Califano, M. Ehrenfeld, and S. Otto, Fluorescence based characterization of early oral squamous cell carcinoma using the Visually Enhanced Light Scope technique. J Craniomaxillofac Surg 45 (2017) 1526-1530. **IF 3,1**

[57] B. Palla, **E. Burian**, J.R. Klecker, R. Fliefel, and S. Otto, Systematic review of oral ulceration with bone sequestration. J Craniomaxillofac Surg 44 (2016) 257-64. **IF 3,1**

[58] S. Otto, M. Troeltzsch, **E. Burian**, S. Mahaini, F. Probst, C. Pautke, M. Ehrenfeld, and W. Smolka, Ibandronate treatment of diffuse sclerosing osteomyelitis of the mandible: Pain relief and insight into pathogenesis. J Craniomaxillofac Surg 43 (2015) 1837-42. **IF 3,1**

10. DANKSAGUNG

Hiermit möchte ich mich bei all jenen bedanken, die mich beim Verfassen dieser Arbeit unterstützt haben. Ich bedanke mich bei dem Klinikdirektor der Poliklinik für Konservierende Zahnheilkunde und Parodontologie der Ludwig-Maximilians-Universität München, Herrn Prof. Dr. med. dent. Reinhard Hickel/ Prof. Dr. med. dent. Falk Schwendicke für die Möglichkeit die vorliegende Promotion an seinem Lehrstuhl durchzuführen.

Mein großer Dank gilt meinem Betreuer, Herrn Prof. Dr. med. Dr. med. dent. Matthias Folwaczny. Ich schulde ihm meine Dankbarkeit, nicht nur für die Überlassung des Themas dieser Dissertation, sondern auch für die allzeit tatkräftige Hilfe bei allen Problemen, die im Laufe der Arbeit auftraten.

Darüber hinaus möchte ich mich bei allen Mitarbeitern des Labors für MR Physik des Instituts für Radiologie der Technischen Universität München unter der Leitung von Prof. Dr. Karampinos bedanken.

Meiner Frau und meinen Eltern gilt ein ganz besonderer Dank. Sie unterstützen mich in allen meinen Entscheidungen aus vollen Kräften und mit aller Liebe. Dadurch war es mir erst möglich diese Arbeit zu erstellen.

11. ADDENDUM – ORIGINALARBEITEN

Clinical Oral Investigations
https://doi.org/10.1007/s00784-023-05159-z

RESEARCH

Evaluation of 3D MRI for early detection of bone edema associated with apical periodontitis

Georg C. Feuerriegel[1] · Egon Burian[1,2,3] · Nico Sollmann[2,3,4] · Yannik Leonhardt[1] · Gintare Burian[5] · Magdalena Griesbauer[2] · Caspar Bumm[6] · Marcus R. Makowski[1] · Monika Probst[2] · Florian A. Probst[6] · Dimitrios C. Karampinos[1] · Matthias Folwaczny[6]

Received: 9 February 2023 / Accepted: 11 July 2023

Abstract

Objectives To detect and evaluate early signs of apical periodontitis using MRI based on a 3D short-tau-inversion-recovery (STIR) sequence compared to conventional panoramic radiography (OPT) and periapical radiographs in patients with apical periodontitis.

Materials and methods Patients with clinical evidence of periodontal disease were enrolled prospectively and received OPT as well as MRI of the viscerocranium including a 3D-STIR sequence. The MRI sequences were assessed for the occurrence and extent of bone changes associated with apical periodontitis including bone edema, periradicular cysts, and dental granulomas. OPTs and intraoral periapical radiographs, if available, were assessed for corresponding periapical radiolucencies using the periapical index (PAI).

Results In total, 232 teeth of 37 patients (mean age 62±13.9 years, 18 women) were assessed. In 69 cases reactive bone edema was detected on MRI with corresponding radiolucency according to OPT. In 105 cases edema was detected without corresponding radiolucency on OPT. The overall extent of edema measured on MRI was significantly larger compared to the radiolucency on OPT (mean: STIR 2.4±1.4 mm, dental radiograph 1.3±1.2 mm, OPT 0.8±1.1 mm, P=0.01). The overall PAI score was significantly higher on MRI compared to OPT (mean PAI: STIR 1.9±0.7, dental radiograph 1.3±0.5, OPT 1.2±0.7, P=0.02).

Conclusion Early detection and assessment of bone changes of apical periodontitis using MRI was feasible while the extent of bone edema measured on MRI exceeded the radiolucencies measured on OPT.

Clinical relevance In clinical routine, dental MRI might be useful for early detection and assessment of apical periodontitis before irreversible bone loss is detected on conventional panoramic and intraoral periapical radiographs.

Keywords Magnetic resonance imaging · Periodontal disease · Root canal · Periapical osteolysis

Abbreviations

2D	Two-dimensional
3D	Three-dimensional
AP	Apical periodontitis
CBCT	Cone beam computed tomography
CT	Computed tomography
FFE	Fast field echo
ICC	Intraclass correlation coefficient
MD	Mean difference
MRI	Magnetic resonance imaging
OPT	Conventional panoramic radiography
PACS	Picture archiving and communication system
PAI	Periapical index
STIR	Short tau inversion recovery
TE	Echo time
TR	Repetition time

Georg C. Feuerriegel and Egon Burian contributed equally to this work.

✉ Georg C. Feuerriegel
georg.feuerriegel@tum.de

Extended author information available on the last page of the article

Introduction

Apical periodontitis (AP) is an inflammatory process caused by pathogens and their toxins occupying the root canal system, and it is commonly initiated by either trauma, caries, or tooth wear [1, 2]. It starts with a non-specific inflammatory reaction in the periapical region of an infected tooth, followed

Published online: 18 July 2023

by a specific innate and adaptive immunological response [3]. The complex interaction of inflammatory cells with numerous biochemical mediators, microbial products, and toxins finally establishes the periradicular pathosis, which can lead to periapical bone resorption and distinctive radiolucencies seen on dental radiography [2, 3]. Moreover, AP mostly presents either as an acute/symptomatic or chronic/asymptomatic disease and histopathologically, the majority of apical periodontitis can be classified into periapical cysts, granulomas, or periapical abscesses, which all appear radiolucent on periapical radiographs [4, 5]. Early treatment of AP is essential as untreated infections are associated with loss of teeth and reduced quality of life as well as, in severe cases, with cellulitis and osteomyelitis [6, 7]. Furthermore, undetected AP constitutes a permanent low-grade infection and is associated with increased risk for cardiovascular diseases [7]. With an individual prevalence of up to 52%, which rises up to 62% for patients over the age of 60 years, AP represents a widespread and most likely underestimated issue with relevant socioeconomic burden due to the high treatment costs [1, 8].

The most established treatment for AP includes root canal treatment, which generally shows good outcome but failure rates of up to 14–16% have been reported, representing a large number in regard to the high prevalence, making prevention as well as early detection highly necessary [2, 9]. So far, the diagnostic approach for AP includes a thorough anamnesis, clinical examination, and radiographic evaluation either using dental radiography, oral panoramic radiography (OPT), or cone beam computed tomography (CBCT) [10]. Conventional radiography offers appropriate sensitivity regarding the detection of periapical radiolucency but only low specificity compared to CBCT, which in turn offers a high sensitivity and specificity but with the downside of exposing the patient to ionizing radiation [11].

In clinical radiology, magnetic resonance imaging (MRI) has been used for more than 20 years for detection of acute and chronic inflammatory changes in bones, musculature, and the gastrointestinal system [12, 13]. Recently, literature on the detection of bone edema using MRI to generate markers for subtle inflammatory intraosseous changes in the alveolar bone but also in the gingiva is increasing [14–19]. Probst et al. showed that intraosseous edema is strongly associated with the severity of inflammatory activity in generalized periodontitis, mirrored by clinical parameters like bleeding on probing or attachment loss [20]. Integrating MRI in the clinical workflow not only for detection of periodontitis but also for clinically silent apical inflammation in the form of circumscribed bone edema would be another step towards dental primary prevention.

Therefore, the aim of this study was to detect and evaluate early signs of AP with edematous changes within the alveolar bone using 3T MRI based on a three-dimensional (3D) short tau inversion recovery (STIR) sequence, and to compare findings with conventional OPT and periapical radiographs in patients with periodontal disease. Our goal was to review the potential of MRI for the detection of early inflammatory processes in the bone. The null hypothesis was that MRI could not generate additional findings regarding the severity and extent of periapical changes in asymptomatic patients compared to radiation-based conventional imaging.

Materials and methods

Patient selection

Patients with clinical evidence of periodontal disease who presented at the Department of Periodontology, Ludwig-Maximilians-University Munich, were enrolled prospectively between March 2018 and April 2019. In total, 232 teeth of 37 patients (mean age 62 ± 13.9 years, 18 women) were assessed. All patients were clinically evaluated by dentists. Clinical findings were not available to the MRI examiners, nor were the results of MRI available to clinical examiners.

The study was conducted according to the STROBE guidelines for observational studies [21]. All procedures were conducted according to the principles expressed in the Declaration of Helsinki. Written patient consent was obtained. The prospective analysis was approved by our institutional review boards (Technical University of Munich: Ref.-No.185/18 S and Ludwig-Maximilians-University Munich: Ref.-No. 18-657). The study was retrospectively registered at the DRKS (German Clinical Trials Register, DRKS00020761).

MRI acquisition

All subjects were examined using a 3T MRI scanner (Ingenia; Philips Healthcare, Best, The Netherlands) with a dedicated 16-channel head-neck and spine coil (dStream Head Neck Spine coil, Philips Healthcare, Best, The Netherlands). The following sequences were acquired: (1) a 3D STIR sequence with the following parameters: echo time (TE), 184 ms; repetition time (TR), 2300 ms; acceleration factor, 2.5; voxel size (acquisition), 0.65 × 0.65 × 1.0 mm^3; slice number, 180; acquisition time, 6.03 min; and (2) a 3D isotropic fast field echo (FFE) T1-weighted black bone sequence with the following parameters: acquisition time, 5:31 min; acquisition voxel size, 0.43 × 0.43 × 0.43 mm^3; TR, 10 ms; TE, 1.75 ms; compressed sense; reduction, 2.3; gap, −0.25 mm; water-fat shift (pix)/bandwidth (Hz), 1503/289. The sequences were acquired in axial orientation and reformatted in sagittal and coronal orientation.

All subjects were examined using a 3-Tesla MRI scanner (Ingenia; Philips Healthcare, Best, The Netherlands) with a dedicated 16-channel head, neck, and spine coil (dStream Head Neck Spine coil, Philips Healthcare, Best, The Netherlands). A 3D short tau inversion recovery (STIR) sequence was acquired with the following parameters: echo time, 184 ms; repetition time, 2300 ms; compressed sensitivity encoding (compressed SENSE) with reduction factor of 2.5; voxel size (acquisition), $0.65 \times 0.65 \times 1.0$ mm^3; slice number, 180, acquisition time, 6.03 min; the sequence was acquired in axial orientation and reformatted in sagittal and coronal orientation.

OPT and dental radiography

All subjects were examined using a two-dimensional (2D) X-ray device (Orthopos S 2D; Dentsply Sirona, Charlotte, NC, USA). The exposure time for the OPT was set for 14.1 s with the following further settings: 63 kV, 8 mA, and FDP 91. Periapical radiographs were made with an intraoral X-ray unit (Heliodent DS; Dentsply Sirona, Charlotte, NC, USA) with an exposure time between 0.03 and 0.06 s depending on the examined tooth. Further settings were as follows: 60mA, 7 mA, and FDP 9-12. Image acquisition was performed using the paralleling technique in which the film is placed parallel to the long axis of the tooth.

Image analysis

The 3D STIR sequences were assessed for the occurrence and extent of bone changes associated with AP including edematous changes to the alveolar bone, periradicular cysts, and dental granulomas. The 3D STIR sequences were reconstructed in three orientations (transversal, sagittal, and coronal) and the maximal extent of the bone edema was measured in millimeters. OPTs and periapical radiographs, if available, were assessed for corresponding periapical radiolucencies using a modified periapical index (PAI) score ranging from 1 – healthy to 5 – severe periapical osteolysis with exacerbating features derived from CBCT according to Gürhan et al. [22]. Furthermore, the maximal extent of the periapical radiolucency was measured.

All image analyses (MRI, periapical radiographs and OPTs) were performed by a radiologist (rater 1, MD with 4 years of experience) and by a dentist and radiologist (rater 2, MD, DMD with 7 years of radiological and 2 years of oral surgery experience). In case of severe artifacts due to metallic restorations or movement artifacts, single teeth were excluded from further analysis. The images were rated individually and independently in random order and blinded to clinical or other diagnostic information. Image analyses were performed on a picture archiving and communication system (PACS) workstation certified for clinical use (IDS7 21.2; Sectra, Linköping, Sweden). The MRI and OPT images were read with an interval of at least 8 weeks in between readings, respectively. For intra-reader agreement, 10 patients were assessed once again after 8 weeks by both raters. A standard five-point Likert scale (1=poor, 2=below average, 3=fair, 4=good, 5=excellent) was used for grading of the diagnostic confidence, as well as the overall image quality. The visibility of AP and the radiolucency on OPT and dental radiograph as well as the bone edema on MRI were also graded using a five-point Likert scale based on the extent of the partial volume effect, blurring, image noise, signal inhomogeneity and discrimination from adjacent structures [23].

Statistics

Findings between the modalities were assessed using Wilcoxon signed-rank tests. Inter- and intra-reader agreements were evaluated with weighted Cohen's κ for ordinal data and intraclass correlation coefficient (ICC) for nominal measurements. Descriptive statistics were performed using paired t-tests (for numeric variables) and McNemar's tests (for binary categorical variables). All statistical tests were performed two-sided and a level of significance (α) of 0.05 was used. The data were analyzed using IBM SPSS Statistics for Windows (version 27.0; IBM Corp., Armonk, NY, USA).

Results

Patient characteristics and API scores

In total, 232 teeth of 37 patients (mean age 62 ± 13.9 years, 18 women) were assessed. Of those, 84 teeth (36%) have been endodontically treated and 148 teeth (64%) have been included without prior treatment. In 174 cases (75%), a reactive bone edema was detected on MRI by both raters (κ 1.00, 95% confidence interval 1.00–1.00) with 69 cases (30%) showing a corresponding radiolucency on OPT (Figs. 1 and 2). In none of the cases, a radiolucency was detected on the OPT without a related bone edema on MRI.

The overall PAI scores measured on the 3D STIR images were significantly higher compared to the PAI scores measured on OPT (rater 1 STIR 2.0 ± 0.3, OPT 1.1 ± 0.7, $P = 0.02$; rater 2 STIR 1.9 ± 1.0, OPT 1.3 ± 0.8, $P = 0.02$, Table 1). Regarding the extent of the bone edema measured on MRI and the corresponding radiolucencies on the OPT, a significantly larger extent was measured on MRI by both raters (rater 1 STIR 2.4 ± 1.6 mm, OPT 0.7 ± 1.1 mm, *P= 0.01*; rater 2 STIR 2.5 ± 1.4 mm, OPT 0.8 ± 1.2 mm, *P= 0.02*). Periapical radiographs were only available in 81 cases (35%), and compared to the 3D STIR, the extent of the bone edema as well as the PAI scores was significantly smaller (bone edema rater 1 STIR 2.4 ± 1.6 mm, dental radiograph

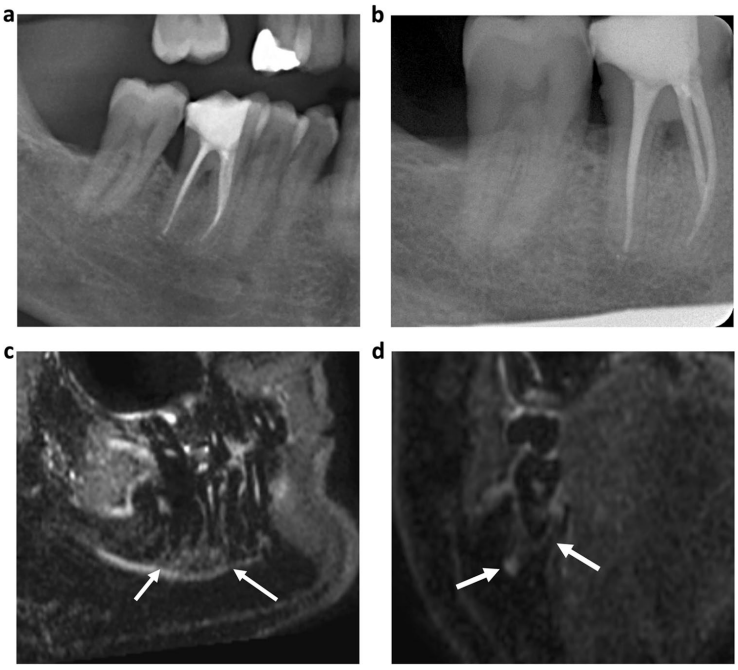

Fig. 1 64-year-old patient with known periodontitis. **a** OPT and **b** dental radiograph of the tooth 46 after root canal treatment showing no distinct radiolucency. **c** Sagittal and **d** coronal reconstruction of a 3D STIR sequence showing a bright edema periapical around the root of the treated tooth. The alveolar bone edema on MRI (white arrows) indicates an inflammatory process but might be also associated with physiological changes. Therefore, findings have to be evaluated together with the results from patient anamnesis and clinical examination

1.1 ± 1.0 mm, $P = 0.03$; rater 2 STIR 2.5 ± 1.4 mm, dental radiograph 1.4 ± 1.3 mm, *P=0.02*; API score rater 1 STIR 2.0 ± 0.3, dental radiograph 1.3 ± 0.4, $P = 0.03$; rater 2 STIR 1.9 ± 1.0, dental radiograph 1.2 ± 0.6, $P = 0.02$).

PAI scores and edema on endodontically and non-treated teeth

The overall PAI scores measured on the 3D STIR images of the endodontically treated teeth were significantly higher compared to the PAI scores measured on OPT and periapical radiographs (rater 1 STIR 1.9 ± 0.7, dental radiograph 1.2 ± 0.3, OPT 1.1 ± 0.2, $P = 0.01$; rater 2 STIR 1.8 ± 0.8, dental radiograph 1.1 ± 0.4, OPT 1.1 ± 0.3, $P = 0.01$). Similar results were obtained for the non-treated teeth (rater 1 STIR 2.3 ± 0.7, dental radiograph 1.3 ± 0.7, OPT 1.2 ± 0.9, $P = 0.04$; rater 2 STIR 2.0 ± 0.9, dental radiograph 1.2 ± 0.5, OPT 1.1 ± 0.5, $P = 0.03$).

The overall extent of the bone edema of the endodontically treated teeth measured on MRI was also significantly larger compared to the radiolucencies measured on OPT and periapical radiographs (rater 1 mean STIR 2.2 ± 0.6 mm, dental radiograph 1.1 ± 0.5 mm, OPT 0.9 ± 0.9 mm, $P = 0.04$; rater 2 mean STIR 2.3 ± 0.9 mm, dental radiograph 1.2 ± 0.3 mm, OPT 0.7 ± 2.3 mm, $P = 0.03$), which was similar for the non-treated teeth (rater 1 STIR 2.6 ± 1.2 mm, dental radiograph 1.2 ± 0.7 mm, OPT 1.1 ± 0.9 mm, $P = 0.01$; rater 2 STIR 2.2 ± 0.9 mm, dental radiograph 1.0 ± 0.8 mm, OPT 0.9 ± 1.1 mm, $P = 0.01$) (Fig. 3).

Visibility of the apical periodontitis and bone edema and diagnostic confidence

The overall image quality of the 3D STIR images as well as OPT images was rated equally good with no significant differences (rater 1 STIR 4.1 ± 0.6, dental radiograph 3.8 ± 0.6, OPT 3.6 ± 0.4, $P = 0.32$; rater 2 STIR 4.2 ± 0.4, dental radiograph 3.9 ± 0.2, OPT 3.8 ± 0.2, $P = 0.66$, Table 2). The diagnostic confidence was overall good for both modalities with no significant differences (rater 1 STIR 3.9 ± 0.4, dental radiograph 3.8 ± 0.5, OPT 3.7 ± 0.3, $P = 0.56$; rater 2 STIR 4.1 ± 0.3, dental radiograph 3.9 ± 0.2, OPT 3.9 ± 0.2, $P = 0.76$).

The visibility of the bone edema was rated significantly better on MRI compared to radiolucency on OPT (rater 1 STIR 4.8 ± 0.7, dental radiograph 2.7 ± 0.3, OPT 2.9 ± 0.2, *P = 0.01*; rater 2 STIR 4.7 ± 0.6, dental radiograph 2.9 ± 0.4, OPT 3.0 ± 0.2, *P = 0.03*). MRI was also rated significantly higher regarding the visibility of AP compared to OPT (rater 1 STIR 4.1 ± 0.3, dental radiograph 3.5 ±

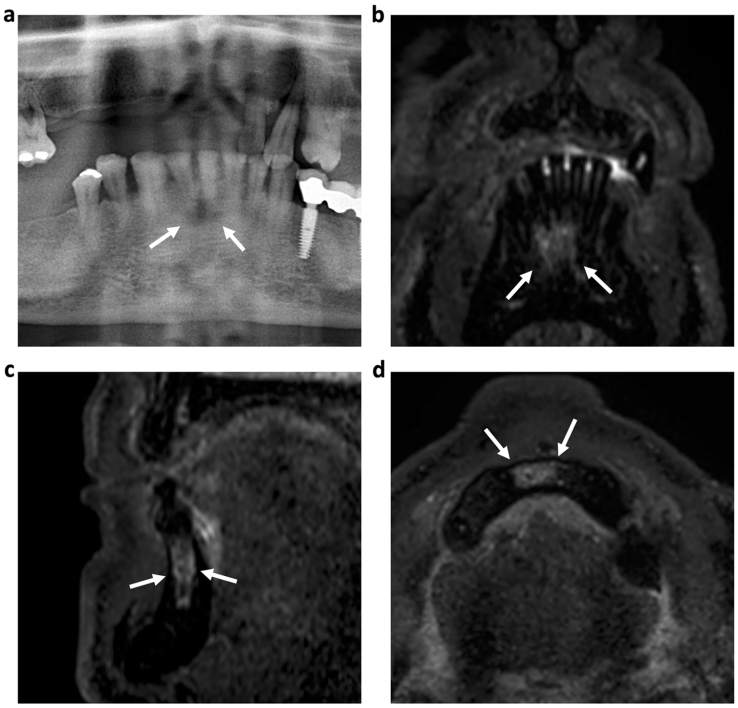

Fig. 2 53-year-old patient with symptomatic periodontitis of the tooth 41. A distinctive periapical radiolucency (white arrows) can be seen on OPT (**a**) and dental radiograph (**b**). The coronal (**c**) and axial (**d**) reconstructions of a 3D STIR sequence show a larger bone marrow edema around the periapical lesion, indicating a larger inflammatory reaction (white arrows)

Table 1 API and edema measurements on MRI and OPT

	OPT	Dental radiograph	3D STIR	*p*-value
Mean extent of radiolucency and bone edema (mm)	0.8±1.1	1.3±1.2	2.4±1.4	0.02
Mean PAI scores	1.2±0.7	1.3±0.5	1.9±0.7	0.03

Data are presented as means ± standard deviations

PAI score OPT and dental radiograph (1= healthy, 5 = severe periapical osteolysis), PAI score MRI (0 = healthy, 5 = diameter of periapical radiolucency > 8 mm)

0.1, OPT 3.2 ± 0.5, $P = 0.01$; rater 2 STIR 3.9 ± 0.3, dental radiograph 3.1 ± 0.4, OPT 3.0 ± 0.2, $P = 0.02$).

Inter- and intra-reader agreement

The inter-reader agreement for the PAI scores measured on the OPT, periapical radiographs, and MRI was substantial to almost perfect (PAI scores OPT: κ 0.95, 95% confidence interval 0.93–1.00; dental radiograph: κ 0.96, 95% confidence interval 0.92–1.00; STIR: κ 0.97, 95% confidence interval 0.94–1.00). A substantial to almost perfect inter-reader agreement was also found for the bone edema (OPT: ICC 0.87, 95% confidence interval 0.83–1.00; dental radiograph: ICC 0.95, 95% confidence interval 0.89–1.00; STIR: ICC 0.94, 95% confidence interval 0.91–1.00). The inter-reader agreement for the visibility of bone marrow edema and periapical radiolucencies was also substantial to almost perfect (κ 0.95, 95% confidence interval 0.90–1.00). For intra-reader agreement, almost all periapical lesions were once more correctly identified by both readers in the 10 patients that were evaluated for this analysis (κ 0.96, 95% confidence interval 0.94–1.00).

Discussion

In this study, detection and assessment of periapical bone edema in clinically silent periapical disease was feasible and accurate compared to standard dental imaging. Furthermore, the extent of the bone edema as well as the PAI scores was significantly higher compared to the measurements on OPT and periapical radiographs. In all patients with periapical radiolucencies on OPT, a corresponding bone edema was

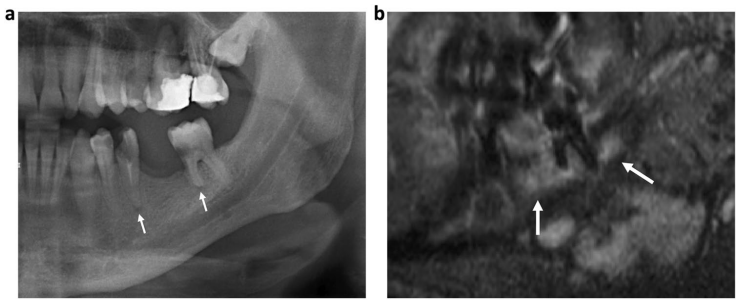

Fig. 3 **a** OPT of a 66-year-old patient with a carious lesion and periodontal disease of the tooth 36. Note the small periapical lesion on the conventional OPT (white arrow). On the sagittal reconstruction of the 3D STIR sequence (**b**), an extensive alveolar bone marrow edema (arrows) is detected which might indicate a markedly larger extent of the inflammation. Compared to MRI, the extent of inflammatory reaction may be underestimated by conventional OPT

Table 2 Qualitative assessments of MRI and OPT

	Reader 1				Reader 2			
	OPT	Dental radiograph	3D STIR	*p*-value	OPT	Dental radiograph	3D STIR	*p*-value
Visibility of radiolucency and bone edema	2.9±0.2	2.7±0.3	4.8±0.7	0.01	3.0±0.2	2.9±0.4	4.7±0.6	0.01
Visibility of periapical lesions	3.2±0.5	3.5±0.1	4.1±0.3	0.01	3.0±0.2	3.1±0.4	3.9±0.3	0.02
Diagnostic confidence	3.7±0.3	3.8±0.5	3.9±0.4	0.56	3.9±0.2	4.0±0.5	4.1±0.3	0.76
Overall image quality	3.6±0.4	3.8±0.6	4.1±0.6	0.32	3.8±0.4	3.9±0.2	4.2±0.2	0.66

Data are presented as means ± standard deviations

5-point Likert scale (5 = best; 1 = worst)

detected on 3D STIR sequences, and the detected bone edema significantly exceeded the measured radiolucency.

So far, detection of AP is commonly achieved using clinical findings in combination with radiographic imaging [2]. For radiographic examination, 2D radiation-based techniques (i.e., intraoral or panoramic radiography) are almost exclusively employed. Due to superimposition of adjacent osseous structures, quality and diagnostic information of 2D images is limited in many cases. However, CT and CBCT can provide 3D images with excellent visualization of hard tissues including the alveolar bone and teeth, but these modalities fail to depict inflammatory processes directly. Additionally, these methods cannot be used as standard procedures in repeated follow-up examinations due to high radiation doses. In contrast, MRI can visualize tooth-related structures including the periodontal ligament with superior resolution and without ionizing radiation. Furthermore, MRI can also depict soft tissue and intraosseous inflammatory changes already at early stages before periapical osteolysis occurs. In this context MRI might be of benefit with regard to detection of initial signs of inflammation.

Geibel et al. recently showed that the assessment of AP using standard T1 and T2 weighted MRI is feasible and accurate compared to CBCT [24, 25]. Furthermore, lesion characterization into e.g. cysts or granulomas was possible and correlated with histopathological findings [24]. However, so far, the surrounding inflammatory reaction and edematous bone changes associated with the periodontal disease as well as AP were not assessed. Yet, Probst et al. were able to show that alveolar bone edema in patients with periodontal disease is associated with the pocket depth in particular over 3 mm and might represent a surrogate marker for the early stages of inflammation before irreversible bone loss has occurred [20]. Yet, they did not assess and compare the extent of the periapical edema and lesions measured on OPT and MRI as well as the effect of endodontic treatment [20]. The magnitude of inflammation is clearly underestimated on conventional dental radiography and OPT [26]. Being able to assess the extent of the osseous inflammation before irreversible bone loss has occurred might improve diagnosis in cases with yet unexplainable persistent odontogenic chronic pain. Moreover, it also might give the physician a better understanding of the time frame in which tooth maintenance or repair has to be achieved.

Furthermore, MRI enables the detection of clinically silent, early stage AP in untreated teeth where no irreversible

osteolysis has occurred yet and, therefore, no radiolucency could be detected on OPT (Fig. 4). Also, the extent of the inflammation could be estimated more realistically, which may lead to more adequate therapy. In endodontically treated teeth, MRI enables monitoring and evaluation of the therapy success. In endodontics, MRI could be used for visualization of chronic inflammation in the form of persistent edematous changes of the bone. After endodontical treatment, a certain risk for bacterial spread over the pulp cavity to the mandibular bone marrow is given as working length of tooth files are chosen to match the apex and over-instrumentation is not performed in daily routine. In these cases, initial or chronic inflammation, which could cause undulating symptoms, could be detected using water-sensitive MRI sequences. Additionally, in contrast to CBCT and OPT, MRI may further allow for differentiation of AP into cysts, granulomas, or abscesses (Fig. 5). Therefore, MRI could represent a suitable radiation-free tool for early detection of

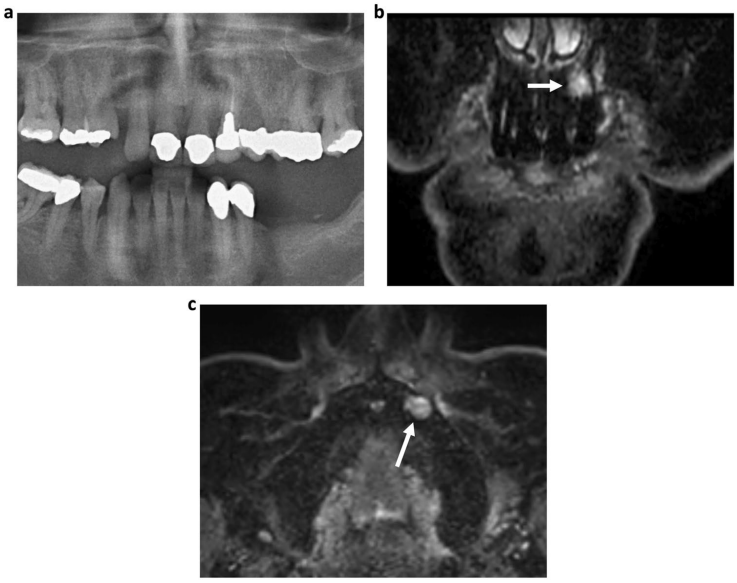

Fig. 4 **a** OPT of a 67-year-old patient with root canal treatment of the tooth 21. Note that the roots of the teeth 12 to 21 are not assessable due to superimposition of the nasal cavity and sinuses. On the coronal (**b**) and axial (**c**) reconstructions of the 3D STIR sequence, a distinct periapical cyst/abscess (white arrows) can be detected next to the root of the tooth 21, which would have been missed on conventional radiography

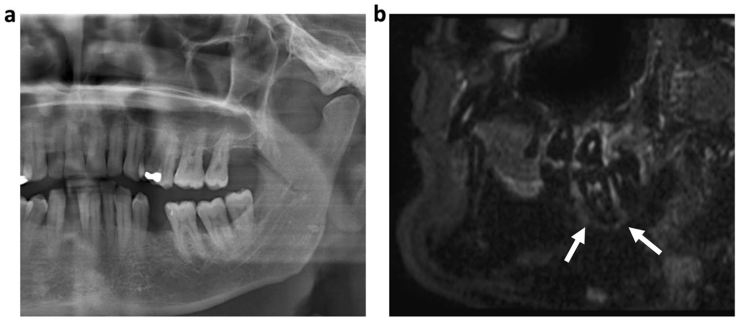

Fig. 5 **a** OPT of a non-symptomatic 58-year-old patient. There are no periapical radiolucencies detected on conventional OPT. In contrast, the sagittal reconstruction of the 3D STIR sequence (**b**) shows a bright periapical bone marrow edema around the root of the tooth 37, indicating the formation of an inflammatory complex that has contact to the adjacent roots (white arrows). The missing radiolucency in the OPT may indicate that it is an early-stage inflammation without osteolysis of the alveolar bone

inflammatory changes as well as for potential short-interval therapy monitoring after endodontic instrumentation.

The aim of this study was not to prove technical superiority of a 3D imaging modality compared to 2D projection radiography. The greater accuracy for cross-sectional imaging like MRI, CBCT, and CT has been proven for several clinical settings before [3, 24, 27]. However, the future potential of MRI for dental use has also been shown and summarized in a recent review by Fluegge et al. [28]. In this context, our results emphasize an expanding indication spectrum for MRI in dentistry for capturing otherwise concealed pathophysiological changes of yet unknown significance. With regard to future trends of AI-based reconstruction and associated scan time reduction and prospective increasing availability of dental dedicated MRI for clinical use, further prospective studies are needed to investigate on this modality and compare it to diagnostic gold standards.

Furthermore, the comparison of MRI using bone-specific sequences like the UTE or ZTE and water-sensitive sequences like the STIR-sequence and CBCT as the current gold standard of visualization of complex dental and periapical anatomy would be of clinical interest. Subsequent prospective studies might further pursue the presented idea of generating complementary diagnostic information in context of endodontic pathology detection and therapy monitoring using MRI compared to CBCT.

There are certain limitations to this study which need to be addressed. First of all, in only one-third of the included patients, a dental radiograph as the current imaging gold standard was available. However, this fact can be explained, as all included patients were asymptomatic with regard to percussion and sensitivity testing. Second, the patient cohort was relatively small and heterogeneous, including patients with and without endodontically treated teeth. Focusing on non-treated teeth might increase the reliability of the results. Another limitation is the prolonged examination time and increased costs of MRI compared to conventional dental radiography, which might be difficult to implement in clinical routine but would reduce radiation exposure to the patient. Evaluation of multi-planar MRI also needs more time and experience compared to the evaluation of OPT and dental radiography, which might limit the use to certain specialized centers, where dentists as well as radiologists work closely together as an interdisciplinary team. Furthermore, considering the used voxel size for MRI, there are partial volume effects which could distort the calculated results to a certain extent, as the spatial resolution of x-ray-based imaging cannot be achieved. No further modalities were available (e.g., histopathological samples) as an external standard of reference, nor were follow-up examinations available to assess the development of bone edema over time. To improve the diagnostic value of MRI, further information on associations between specific histopathological changes and intraosseous edema within the tooth-supporting bone should be obtained. Osseous edema as depicted with STIR sequences is associated histologically with the replacement of bone marrow fat by an inflammatory infiltrate in rheumatoid arthritis [29]. Apart from primary inflammatory conditions (i.e., rheumatoid arthritis or spondyloarthritis), also excessive functional stress might cause osseous edema, which needs to be examined in future studies.

Finally, the high sensitivity of MRI in detecting periapical lesions might not only lead to the detection of lesions that would have been missed on conventional methods but might also lead to the detection of lesions which can be considered temporary and might be self-resolving without any additional treatment needed. In order to avoid unnecessary treatment initiation or overtreatment, detected lesions should always be evaluated together with the results from patient anamnesis and clinical examination.

In summary, we conclude that the early detection and assessment of edematous bone changes of AP using 3D STIR imaging was feasible, while the extent of bone edema measured on MRI exceeded the radiolucencies measured on OPT. In clinical routine, dental MRI might be useful for early detection and assessment of AP before irreversible bone loss can be detected by conventional panoramic and periapical radiographs.

Author contributions All authors contributed to the study conception and design. G.C.F. wrote the main manuscript text and was mainly responsible for the conception and design of the study. Y.L. and N.S. helped draft the article and revised it critically. G.B., M.G., and C.B. helped with data acquisition and analysis. G.C.F. prepared the figures. D.C.K, M.R.M, F.A.P, M.P., and M.F. helped with the conception of the study and the interpretation of results. E.B. contributed substantially to the analysis and interpretation of data as well as the revision of the manuscript. All authors read and approved the final manuscript.

Funding Open Access funding enabled and organized by Projekt DEAL.

Data availability The data are available from the authors upon reasonable request.

Declarations

Ethics approval and consent to participate All procedures were conducted according to the principles expressed in the Declaration of Helsinki. Written informed consent was obtained from all participants prior to inclusion. The prospective analysis was approved by our institutional review boards (Technical University of Munich: Ref.-No.185/18 S and Ludwig-Maximilians-University Munich: Ref.-No. 18-657). The study was retrospectively registered at the DRKS (German Clinical Trials Register, DRKS00020761).

Conflict of interest The authors declare no competing interests.

References

1. Tibúrcio-Machado CS, Michelon C, Zanatta FB, Gomes MS et al (2021) The global prevalence of apical periodontitis: a systematic review and meta-analysis. Int Endod J 54(5):712–735
2. Karamifar K, Tondari A, Saghiri MA (2020) Endodontic periapical lesion: an overview on the etiology, diagnosis and current treatment modalities. Eur Endod J 5(2):54–67
3. Cotti E, Schirru E (2022) Present status and future directions: imaging techniques for the detection of periapical lesions. Int Endod J 55:1085–1099
4. Lalonde ER, Luebke RG (1968) The frequency and distribution of periapical cysts and granulomas. An evaluation of 800 specimens. Oral Surg Oral Med Oral Pathol 25(6):861–868
5. Shteyer A, Rozovsky E (1972) Periapical lesions--types, incidence and clinical features. Refuat Hapeh Vehashinayim 21:100–103
6. Parrish LC, Kretzschmar DP, Swan RH (1989) Osteomyelitis associated with chronic periodontitis: a report of three cases. J Periodontol 60(12):716–722
7. Sebring D, Buhlin K, Norhammar A, Rydén L et al (2022) Endodontic inflammatory disease: a risk indicator for a first myocardial infarction. Int Endod J 55(1):6–17
8. Figdor D (2002) Apical periodontitis: a very prevalent problem. Oral Surg Oral Med Oral Pathol Oral Radiol Endodontol 94(6):651–652
9. Torabinejad M, Anderson P, Bader J, Brown LJ et al (2007) Outcomes of root canal treatment and restoration, implant-supported single crowns, fixed partial dentures, and extraction without replacement: a systematic review. J Prosthet Dent 98(4):285–311
10. Cotti E (2010) Advanced techniques for detecting lesions in bone. Dent Clin North Am 54(2):215–235
11. Mostafapoor M, Hemmatian S (2022) Evaluation of the accuracy values of cone-beam CT regarding apical periodontitis: a systematic review and meta-analysis. Oral Radiol 38(3):309–314
12. Sempere GA, Martinez Sanjuan V, Medina Chulia E, Benages A et al (2005) MRI evaluation of inflammatory activity in Crohn's disease. AJR Am J Roentgenol 184(6):1829–1835
13. Miller TT, Randolph DA Jr, Staron RB, Feldman F et al (1997) Fat-suppressed MRI of musculoskeletal infection: fast T2-weighted techniques versus gadolinium-enhanced T1-weighted images. Skeletal Radiol 26(11):654–658
14. Juerchott A, Sohani M, Schwindling FS, Jende JME et al (2020) In vivo accuracy of dental magnetic resonance imaging in assessing maxillary molar furcation involvement: a feasibility study in humans. J Clin Periodontol 47(7):809–815
15. Juerchott A, Pfefferle T, Flechtenmacher C, Mente J et al (2018) Differentiation of periapical granulomas and cysts by using dental MRI: a pilot study. Int J Oral Sci 10(2):17
16. Ruetters M, Juerchott A, El Sayed N, Heiland S et al (2019) Dental magnetic resonance imaging for periodontal indication - a new approach of imaging residual periodontal bone support. Acta Odontol Scand 77(1):49–54
17. Juerchott A, Sohani M, Schwindling FS, Jende JME et al (2020) Comparison of non-contrast-enhanced dental magnetic resonance imaging and cone-beam computed tomography in assessing the horizontal and vertical components of furcation defects in maxillary molars: an in vivo feasibility study. J Clin Periodontol 47(12):1485–1495
18. Newbould RD, Bishop CA, Janiczek RL, Parkinson C et al (2017) T2 relaxation mapping MRI of healthy and inflamed gingival tissue. Dentomaxillofac Radiol 46(2):20160295
19. Schara R, Sersa I, Skaleric U (2009) T1 relaxation time and magnetic resonance imaging of inflamed gingival tissue. Dentomaxillofac Radiol 38(4):216–223
20. Probst M, Burian E, Robl T, Weidlich D et al (2021) Magnetic resonance imaging as a diagnostic tool for periodontal disease: a prospective study with correlation to standard clinical findings-Is there added value? J Clin Periodontol 48(7):929–948
21. von Elm E, Altman DG, Egger M, Pocock SJ et al (2007) The Strengthening the Reporting of Observational Studies in Epidemiology (STROBE) statement: guidelines for reporting observational studies. Lancet 370(9596):1453–1457
22. Gurhan C, Sener E, Mert A, Sen GB (2020) Evaluation of factors affecting the association between thickening of sinus mucosa and the presence of periapical lesions using cone beam CT. Int Endod J 53(10):1339–1347
23. Notohamiprodjo M, Kuschel B, Horng A, Paul D et al (2012) 3D-MRI of the ankle with optimized 3D-SPACE. Invest Radiol 47(4):231–239
24. Geibel MA, Schreiber E, Bracher AK, Hell E et al (2017) Characterisation of apical bone lesions: comparison of MRI and CBCT with histological findings - a case series. Eur J Oral Implantol 10(2):197–211
25. Geibel MA, Schreiber ES, Bracher AK, Hell E et al (2015) Assessment of apical periodontitis by MRI: a feasibility study. Rofo 187(4):269–275
26. Estrela C, Bueno MR, Leles CR, Azevedo B et al (2008) Accuracy of cone beam computed tomography and panoramic and periapical radiography for detection of apical periodontitis. J Endod 34(3):273–279
27. Groenke BR, Idiyatullin D, Gaalaas L, Petersen A et al (2023) Sensitivity and specificity of MRI versus CBCT to detect vertical root fractures using microCT as a reference standard. J Endod
28. Flugge T, Gross C, Ludwig U, Schmitz J et al (2023) Dental MRI-only a future vision or standard of care? A literature review on current indications and applications of MRI in dentistry. Dentomaxillofac Radiol 52(4):20220333
29. Jimenez-Boj E, Nobauer-Huhmann I, Hanslik-Schnabel B, Dorotka R et al (2007) Bone erosions and bone marrow edema as defined by magnetic resonance imaging reflect true bone marrow inflammation in rheumatoid arthritis. Arthritis Rheum 56(4):1118–1124

Authors and Affiliations

Georg C. Feuerriegel[1] · Egon Burian[1,2,3] · Nico Sollmann[2,3,4] · Yannik Leonhardt[1] · Gintare Burian[5] · Magdalena Griesbauer[2] · Caspar Bumm[6] · Marcus R. Makowski[1] · Monika Probst[2] · Florian A. Probst[6] · Dimitrios C. Karampinos[1] · Matthias Folwaczny[6]

Egon Burian
egon.burian@tum.de

Nico Sollmann
nico.sollmann@tum.de

Yannik Leonhardt
yannik.leonhardt@tum.de

Gintare Burian
gintare.burian@med.uni-muenchen.de

Magdalena Griesbauer
lena@der-griesbauer.de

Caspar Bumm
caspar.bumm@med.uni-muenchen.de

Marcus R. Makowski
marcus.makowski@tum.de

Monika Probst
monika.probst@tum.de

Florian A. Probst
flo.probst@web.de

Dimitrios C. Karampinos
dimitrios.karampinos@tum.de

Matthias Folwaczny
matthias.folwaczny@med.uni-muenchen.de

[1] Department of Diagnostic and Interventional Radiology, Klinikum rechts der Isar, School of Medicine, Technical University of Munich, Ismaninger Strasse 22, 81675 Munich, Germany

[2] Department of Diagnostic and Interventional Neuroradiology, Klinikum rechts der Isar, School of Medicine, Technical University of Munich, Munich, Germany

[3] Department of Diagnostic and Interventional Radiology, University Hospital Ulm, Ulm, Germany

[4] TUM-Neuroimaging Center, Klinikum rechts der Isar, Technical University of Munich, Munich, Germany

[5] Department of Prosthodontics, LMU University Hospital, Ludwig-Maximilians-University, Munich, Germany

[6] Department of Restorative Dentistry and Periodontology, LMU University Hospital, Ludwig-Maximilians-University, Munich, Germany

Clinical Oral Investigations (2023) 27:3705–3712
https://doi.org/10.1007/s00784-023-04986-4

RESEARCH

Visualization of clinically silent, odontogenic maxillary sinus mucositis originating from periapical inflammation using MRI: a feasibility study

Egon Burian[1,2,3] · Georg Feuerriegel[3] · Nico Sollmann[1,2,4] · Gintare Burian[5] · Benjamin Palla[6] · Magdalena Griesbauer[1] · Caspar Bumm[7] · Monika Probst[1] · Meinrad Beer[2] · Matthias Folwaczny[7]

Received: 20 January 2023 / Accepted: 28 March 2023 / Published online: 11 April 2023

Abstract

Objectives Maxillary sinus mucositis is frequently associated with odontogenic foci. Periapical inflammation of maxillary molars and premolars cannot be visualized directly using radiation-based imaging. The purpose of this study was to answer the following clinical question: among patients with periapical inflammatory processes in the maxilla, does the use of magnetic resonance imaging (MRI), as compared to conventional periapical (AP) and panoramic radiography (OPT), improve diagnostic accuracy?

Methods Forty-two subjects with generalized periodontitis were scanned on a 3 T MRI. Sixteen asymptomatic subjects with mucosal swelling of the maxillary sinus were enrolled in the study. Periapical edema was assessed using short tau inversion recovery (STIR) sequence. Apical osteolysis and mucosal swelling were assessed by MRI, AP, and OPT imaging using the periapical index score (PAI). Comparisons between groups were performed with chi-squared tests with Yates' correction. Significance was set at $p < 0.05$.

Results Periapical lesions of maxillary premolars and molars were identified in 16 subjects, 21 sinuses, and 58 teeth. Bone edema and PAI scores were significantly higher using MRI as compared to OPT and AP ($p < 0.05$). Using the STIR sequence, a significant association of PAI score > 1 and the presence of mucosal swelling in the maxillary sinus was detected ($p = 0.03$).

Conclusion Periapical inflammation and maxillary mucositis could be visualized using STIR imaging. The use of MRI may help detect early, subtle inflammatory changes in the periapical tissues surrounding maxillary dentition. Early detection could guide diagnostic criteria, as well as treatment and prevention.

Keywords Magnetic resonance imaging · Periapical inflammation · Periapical osteolysis · Mucositis

Introduction

The association between periapical inflammation of maxillary dentition and odontogenic sinusitis is well documented [1]. In current clinical practice, the diagnosis of odontogenic maxillary sinusitis is based on the detection of apical osteolysis using radiation-based imaging techniques [2, 3]. Periapical osteolysis is a late-stage outcome following chronic inflammation, often from caries-induced pulpitis or endoperio lesions. Prior to this, lymphocytes and monocytes infiltrate the periapical tissue and initiate an inflammatory cascade of cytokines. These cytokines and mediators disrupt the RANK-RANKL OPG pathway leading to edema [4–8]. The localized edematous change adjacent to the periapical tissues can be visualized using magnetic resonance imaging (MRI) [9].

Current imaging modalities common to clinical practice, such as panoramic radiographs (OPT), periapical radiographs (AP), computed tomography (CT), or cone beam CT (CBCT), allow for visualization of osseous and dental structures with high spatial resolution [10–14]. However, these radiation-based modalities lack the ability to detect intraosseous edema that proceeds bone loss and osteolysis. In contrast, MRI uses water-sensitive imaging sequences that can detect subtle edematous changes. MRI has a higher sensitivity and specificity when compared to radiation-based techniques for detecting periodontal edema and mucositis of the maxillary sinus [15]. In addition, MRI is able to distinguish between mucositis and other infectious etiologies such as empyema, which require different treatments and can lead

✉ Egon Burian
e.burian@gmx.net

Extended author information available on the last page of the article

to severe ascending complications like orbital infection and intracranial abscess formation [16–18]. Recent literature has demonstrated a growing application of MRI for the visualization of dental and osseous structures, all without exposing patients to ionizing radiation [19–24].

There are several fields in dentistry that have utilized MRI. In endodontics, good reproducibility has been shown for visualizing root canals and determining the working length of endodontic files [25, 26]. In periodontics, Probst et al. described water-sensitive STIR sequences to detect bone edema in generalized periodontitis, and Juerchott et al. described the use of MRI for the evaluation of furcation defects [9, 19]. In oral surgery, the use of MRI for implant planning and third molar removal demonstrated good diagnostic accuracy [27–29]. In orthodontics, a recent MRI study showed reliable 3D cephalometric analysis when compared to CBCT [30].

The purpose of this study was to answer the following clinical question: among patients with periapical inflammatory processes in the maxilla, does the use of magnetic resonance imaging (MRI), as compared to conventional periapical (AP) and panoramic radiography (OPT), improve diagnostic accuracy?

Methods

Study design

Forty-two subjects who presented to the Department of Periodontology, Ludwig-Maximilians-University Munich, from May to December 2018 with clinical evidence of periodontal disease were included in this study. All subjects presented with a diagnosis of periodontitis. Clinical findings were not available to the MRI examiners, nor were the results of the MRI available to clinical examiners.

The inclusion criteria were the prevalence of mucosal swelling on the MRI, the availability of an existing OPT, and no symptoms of a sinusitis. Exclusion criteria were recent oral surgery procedures, a history of oral maxillofacial syndromes, and standard contraindications for MRI (e.g., implanted pacemaker). Of the 42 subjects who completed the MRI, 16 subjects fulfilled the described inclusion criteria and were enrolled.

The study received an institutional review board approval (Technical University of Munich: Ref.-No.185/18 S and Ludwig-Maximilians-University Munich: Ref.-No. 18–657). The study was retrospectively registered at the DRKS (German Clinical Trials Register, DRKS00020761).

MRI acquisition

All subjects were scanned with a 3 T MRI scanner (Elition, Philips Healthcare, Best, The Netherlands) at the Department of Diagnostic and Interventional Neuroradiology, Technical University of Munich, using a 16-channel head-neck cervical spine array. Patients were positioned head-first in a supine position. The sequence protocol consisted of a short survey scan for sequence position planning (acquisition time 0:39 min), a three-dimensional (3D) isotropic T2-weighted short tau inversion recovery (STIR) sequence (acquisition time 6:03 min, acquisition voxel size $0.65 \times 0.65 \times 0.65$ mm^3, repetition time (TR) 2300 ms, echo time (TE) 184 ms, inversion recovery (IR) 250 ms, compressed sense, reduction 5, gap – 0.5 mm, slice oversampling 1.5, water-fat shift (pix)/bandwidth (Hz) 1766/246), and a 3D isotropic T1-weighted fast field echo (FFE) black bone sequence (acquisition time 5:31 min, acquisition voxel size $0.43 \times 0.43 \times 0.43$ mm^3, TR 10 ms, TE 1.75 ms, compressed sense, reduction 2.3, gap – 0,25 mm, water-fat shift (pix)/bandwidth (Hz) 1503/289).

The 3D T1-weighted black bone sequence was used for the determination of changes within the tooth-supporting alveolar bone associated with periodontitis. The main sequence used for edema detection within the bone was the 3D STIR sequence.

Analysis of the panoramic radiographs and the periapical radiographs

All OPT and AP imaging was analyzed for the presence of periapical radiolucencies and associated thickening of the maxillary sinus mucosa. For periapical analysis, a periapical index (PAI) score ranging from 1 – healthy, to 5 – severe periapical osteolysis with exacerbating features was used [31] (Table 1).

MRI analysis

The detection and measurement of edema were performed in the 3D T2-weighted STIR sequences. The extent of intraosseous edema was measured from cranial to caudal, from medial to lateral, and from ventral to dorsal. The PAI score was graded using a modified version originally implemented for evaluation on CBCT by Estrela et al. [32] (Table 2). Changes of the bone architecture and osteolysis were evaluated on the 3D T1-weighted black bone sequences.

Table 1 Periapical index (PAI) for panoramic and apical radiographs

PAI	Score definition
1	Normal periapical structures
2	Small changes in bone structure
3	Changes in bone structure with mineral loss
4	Apical periodontitis with well-defined radiolucent area
5	Severe apical periodontitis with exacerbating features

Assessment of the type and extent of mucosal swelling

The thickness of the mucosa lining the inferior aspect of the maxillary sinus was measured in millimeters using the coronal, axial, and sagittal reformations of the 3D T2-weighted STIR and T1-weighted FFE sequences according to Gürhan et al. and Shanbhag et al. [33, 34]: class 1: 2.1–5 mm; class 2: 5.1–10 mm; and class 3: > 10 mm. Qualitatively, the appearance of the mucosa was classified as "flat" (horizontal thickening of the sinus floor mucosa) or "polypoid" (dome-shaped thickening of the sinus floor mucosa). Image analysis was performed by a radiologist (MD with 4 years radiology experience) and a dentist and radiologist (MD and DMD; 7 years radiology experience, 2 years oral surgery experience). In cases of severe artifacts due to metallic restorations or movement artifacts, single teeth were excluded from further analysis.

Statistical analysis

SPSS software version 26.0 (SPSS Inc, Chicago, IL, USA) was used for all statistical tests. For continuous variables, the mean and standard error of the mean (SEM) were calculated. Within each experimental group, the normal distribution of data was tested using the Kolmogorov-Smirnov procedure. The Mann-Whitney test was used for independent variables. For categorial data, absolute numbers and the relative frequency within each group are presented. Group comparisons were performed with chi-squared tests with Yates' correction. Intra- and inter-reader agreements were evaluated. A p-value of <0.05 was considered statistically significant.

Results

Patient cohort and clinical findings

Sixteen of the initial 42 subjects were included in this study according to the inclusion and exclusion criteria described in the "Methods" section (mean age 58 years; age range 28–82 years, 10 men and 6 women) with 58 affected teeth.

Table 2 Modified periapical index (PAI) for magnetic resonance imaging

PAI	Score definition
0	Intact periapical structure
1	Diameter of periapical radiolucency > 0.5–1 mm
2	Diameter of periapical radiolucency > 1.1–2 mm
3	Diameter of periapical radiolucency > 2.1–4 mm
4	Diameter of periapical radiolucency > 4.1–8 mm
5	Diameter of periapical radiolucency > 8 mm

Dental findings in panoramic radiographs and dental apical radiographs

Of the 58 teeth, alterations in periapical alveolar bone were detected in 23 teeth using OPT and 24 using AP. No significant association was detected for the extent of apical lesion (neither with a PAI of ≤ 2 nor with a PAI of ≥ 2) or the presence of mucosal swelling ($p > 0.05$). No significant difference was detected on AP films for PAI of 1 compared to PAI of > 1 ($p > 0.05$). For conventional imaging technique, no significant correlation was identified between PAI and mucosal swelling.

Dental findings on MRI

Using the STIR sequence, a significant association of a PAI score > 1 and the presence of mucosal swelling in the maxillary sinus was detected ($p = 0.03$). However, the extent and type of mucosal swelling revealed no statistically significant association with the PAI score detected on MRI. For example, Fig. 1 displays subtle periapical edema at the buccal roots of a second molar associated with flat mucosal thickening. Figure 2 displays an extensive apical granuloma that can be seen on the STIR sequence with associated subtle bone edema. Descriptive findings are given in Table 3.

Mucosal pathologies detected on MRI

In 16 subjects, 21 maxillary sinuses demonstrated mucosal swelling. The predominant type of mucosal swelling was the flat type (18 of 21 maxillary sinuses), whereas only 3 subjects showed a polypoid configuration. In eight subjects, the bottom thickness of the maxillary mucosa could be classified as class 1, in 4 subjects the thickness corresponding to class 2, and in 9 subjects the thickness corresponded to more than 10 mm (class 3).

In OPT as well as in AP, only two subjects with class 1 thickness were detected. Half of the cases assigned to class 2 were detected on both conventional radiation-based imaging techniques.

Intra- and inter-reader agreement

The inter-reader agreement for the PAI scores on the OPT, dental radiographs, and MRI was substantial to almost perfect (OPT: κ 0.94, 95% confidence interval 0.93–1.00; dental radiograph: κ 0.96, 95% confidence interval 0.92–1.00; 3D STIR κ 0.95, 95% confidence interval 0.94–1.00). The inter-reader agreement for the detection of mucosal swelling was also substantial to almost perfect (κ 0.93, 95% confidence

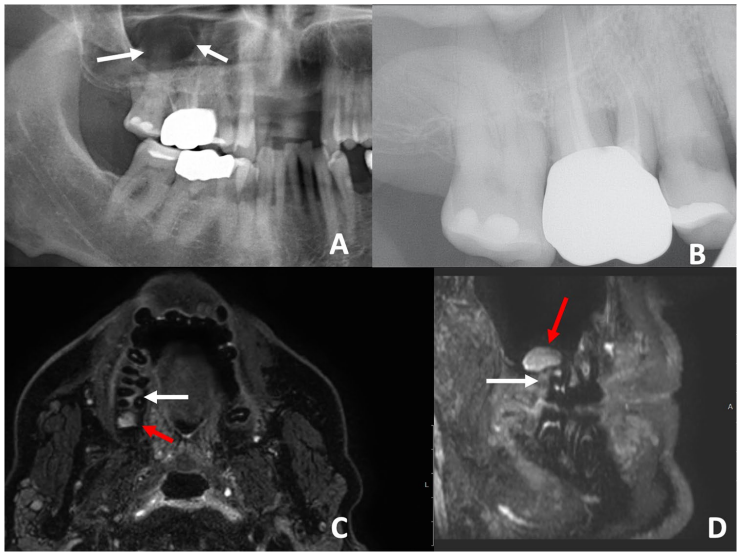

Fig. 1 **A** OPT with close spatial relation between the roots of the endodontically treated tooth 16 and the tooth 17. The right maxillary sinus appears to be normal. A circumscribed radiolucency can be seen in the maxillary sinus (white arrows). **B** AP with subtle periodontal space widening around the disto-buccal and the palatinal roots of tooth 17 and the mesio-buccal root of tooth16. **C** In the coronal slice of the STIR sequence, a subtle flat mucosal swelling cranial to the tooth 16 can be detected (red arrow). **D** The sagittal slice shows a subtle STIR-hyperintense bone edema that can be seen distal to the disto-buccal root and in the region of the furcation of tooth 17 (white arrow). The mucosal swelling can be detected at the floor of the maxillary sinus (red arrow)

interval 0.90–1.00). For intra-reader reliability, both readers reassessed the images of 10 patients after at least 8 weeks, showing very good agreement between the two time points (κ 0.97, 95% confidence interval 0.94–1.00).

Discussion

In this study, we showed that periapical edema of maxillary molars and premolars detected on MRI was associated with the presence of mucosal thickening of the maxillary sinus. Notably, pathological periapical findings on MRI were not significantly associated with the severity of inflammatory reaction. However, subtle changes of PAI could be detected by MRI, prior to the onset of osteolysis that would be detectable on conventional radiography. Thus, MRI seems to be suitable for the early detection of periapical changes with associated mucosal swelling that are not present on OPT or AP.

This project sought to compare MRI, which is considered to be an advanced imaging modality, to standard-of-care imaging that is routinely available in a dental office. In more advanced surgical or hospital-based settings, the use of CT and CBCT are also available to analyze more precise anatomical structures in demanding clinical situations [10–12, 35]. The downside of all X-ray-based imaging techniques is the individual's exposure to ionizing radiation harboring the risk of stochastic radiation effects with associated damage of the deoxyribonucleic acid (DNA). That being said, every clinician should follow the ALARA principle ("as low as reasonably achievable") when making the choice for an imaging technique [24].

In contrast to radiation-based imaging techniques, MRI is based on non-ionizing radiation using the different magnetic properties of hydrogen nuclei contained in water and fat for generating images. This is the reason why MRI is able to depict soft tissues with a much higher contrast than conventional cross-sectional imaging modalities. Recently, Van der Cruyssen et al. and Juerchott et al. have shown that by optimizing sequence protocols, direct visualization of small trigeminal branches and even complex structures like the dental pulp is possible, which improves our understanding of nerve physiology in vivo [36–39]. Furthermore, using T1-based imaging or ultrashort or zero echo time sequences, even the visualization of hard tissues like the mandibular bone and pathological alterations in the course of periodontitis or osteonecrosis has been feasible [9, 27, 40, 41].

STIR imaging has been proven to detect bone edema as a marker for inflammatory changes in hard and soft tissue [42, 43]. Hyperintense signal alterations using STIR sequences can detect changes to the osseous matrix even before T1-weighted sequences. By applying STIR sequences to dental medicine, apical inflammation that was previously undetectable on X-ray imaging and clinically silent can now be detected. The early identification of these inflammatory processes could allow intervention

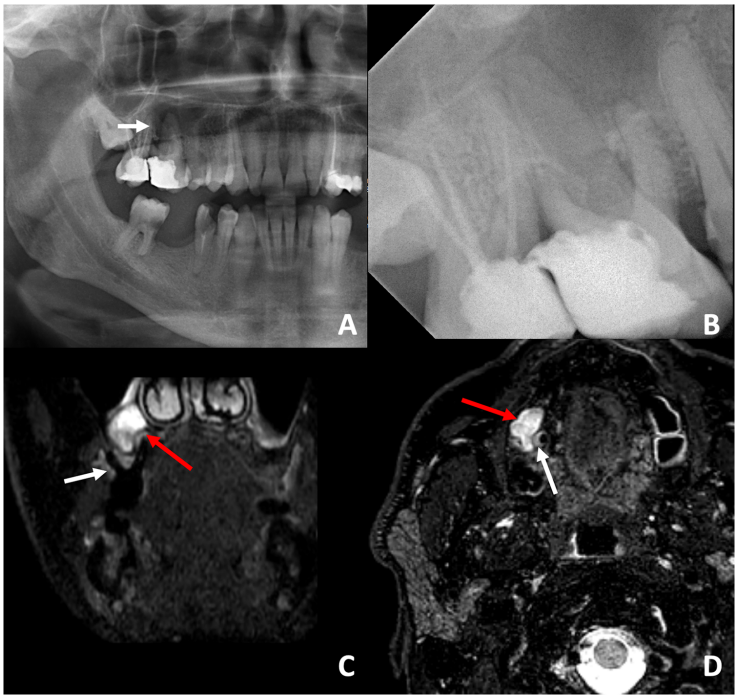

Fig. 2 **A** OPT with impression of a periapical radiolucency around the mesio-buccal root of tooth 16 (white arrow). However, artificial air superimposition would also be a differential diagnosis. **B** The AP shows subtle changes around the mesio-buccal and the palatal roots of tooth 16. The endodontically treated tooth 17 also has a widened periodontal ligament space around the mesio-buccal root. Root canal treatment appears sufficient. **C** In the STIR sequence (coronal slice), a large bone edema around the mesio-buccal of tooth 16 can be detected (white arrow), exceeding the corresponding radiolucency displayed in the AP. Additionally, a marked STIR-hyperintense, periapical granuloma is depicted and lifts the Schneiderian membrane more cranial (STIR-hypointense, linear structure, white arrow). Above the Schneiderian membrane, a mucosal swelling can be detected (red arrow). **D** In the axial slice, the full extent of the STIR-hyperintense bone edema (white arrow) can be delineated. The bottom part of the granuloma can be seen (red arrow)

Table 3 PAI and edema measurements on MRI and OPT

Overall				
	OPT	Dental radiograph	3D STIR	*p*-value
Mean extent of radiolucency and bone edema (mm)	1.3 ± 1.6	0.8 ± 1.8	2.4 ± 1.5	< 0.05
Mean PAI scores	2.1 ± 0.7	1.8 ± 0.5	2.1 ± 0.6	< 0.05

Data are presented as means ± standard deviations

PAI score OPT and dental radiograph (1 = healthy, 5 = severe periapical osteolysis), PAI score MRI (0 = healthy, 5 = diameter of periapical radiolucency > 8 mm)

prior to exacerbations and chronic disorders. Furthermore, follow-up imaging with close intervals is possible to validate the suspected diagnosis and monitor progression.

In a recent study, STIR sequences were utilized to detect bone edema and showed a good correlation to clinical parameters in periodontitis [9]. The authors previously attempted to raise clinician awareness to MRI capabilities in detecting early osseous and inflammatory changes related to odontogenic infections. A survey among otolaryngology residents conducted in the USA showed

that there is a lack of knowledge in regard to odontogenic sinusitis, which can have serious risks ranging from orbital infections to intracranial spread [2, 16, 18]. In this context, applying MRI in a clinical setting using dedicated water-sensitive sequences could help identify teeth at risk or with already detectable edema before inflammatory spread to other anatomic structures. Thus, MRI can depict soft tissue and intraosseous inflammatory changes in early stages, which gives clinicians the opportunity to review treatment options [9, 44]. In cases of associated tooth decay, timely initiation of excavation with subsequent partial pulpotomy or pulpectomy could prevent bacterial spread to the alveolar bone and shorten intervals to definitive root canal filling. However, there are certain settings that hamper the specificity of detected hyperintensities derived from STIR sequences. Patients with parafunctions and bruxism not only exhibit dental attrition, but also expose the periodontium and the adjacent alveolar bone to pathological loading, which might be mirrored by periapical signal alterations. For interpreting the obtained images of MRI, advanced knowledge of anatomy and sequence peculiarities is essential, which requires a good communication of the clinician and the radiologist to maximize diagnostic accuracy and improve patient treatment.

This study supports the use of MRI as a complementary imaging modality in the clinical evaluation of periapical inflammatory changes. It has to be stated that for optimal diagnostic quality, the combination of MRI and conventional radiography is mandatory depending on dental examination and derived indication. For direct visualization of osseous and dental structures and pathologies OPT, AP and bitewing imaging is and will be essential in dental diagnostics.

The conducted study has several limitations. As a feasibility study limited to a small cohort, the *n* value was small and did not allow for advanced statistical analysis. The presented results are limited and need to be validated in larger cohorts. Second, in subjects that have subtle changes of the mucosal thickness, artifacts arising from the air-filled maxillary sinus can reduce image quality. Third, although the applied sequence protocol was rather short, image quality could be hampered by motion (e.g., chewing or mouth breathing).

Conclusion

Periapical inflammation and maxillary mucositis could be visualized using STIR imaging. The use of MRI may help detect early, subtle inflammatory changes in the periapical tissues surrounding maxillary dentition. Early detection could guide diagnostic criteria, as well as treatment and prevention.

Acknowledgements We thank the study participants for their commitment to this study.

Author contribution EB, MP, and MF contributed to the study conception and design, to data acquisition, to data analysis and interpretation, and to the writing and revision of the manuscript. NS, GF, CB, GB, MB, and MG contributed to data acquisition, to data analysis and interpretation, to the writing and revision of the manuscript, to the study conception and design, to data interpretation, and to the writing and revision of the manuscript. All authors reviewed and approved the final version of the manuscript and agreed to be accountable for all aspects of work ensuring integrity and accuracy.

Funding Open Access funding enabled and organized by Projekt DEAL. MRI examinations of this project were covered by in-house funds of the Department of Diagnostic and Interventional Neuroradiology, Klinikum rechts der Isar, Technical University of Munich, Munich, Germany. The authors did not receive any other financial or material support.

Data availability All source data are stored at the Department of Neuroradiology, Technical University of Munich, Munich, Germany. We invite parties interested in collaboration and data exchange to contact the corresponding author directly.

Declarations

Ethics approval and consent to participate The study received institutional review board approval (Technical University of Munich: Ref.-No.185/18 S and Ludwig-Maximilians-University Munich: Ref.-No. 18–657). All participants gave written informed consent to the study.

Consent for publication Not applicable.

Competing interests The authors declare no competing interests.

References

1. Craig JR (2022) Odontogenic sinusitis: a state-of-the-art review. World J Otorhinolaryngol Head Neck Surg 8(1):8–15
2. Shukairy MK et al (2020) Recognizing odontogenic sinusitis: a national survey of otolaryngology chief residents. Am J Otolaryngol 41(6):102635
3. Whyte A, Boeddinghaus R (2019) Imaging of odontogenic sinusitis. Clin Radiol 74(7):503–516
4. Stashenko P, Teles R, D'Souza R (1998) Periapical inflammatory responses and their modulation. Crit Rev Oral Biol Med 9(4):498–521
5. Takahama A Jr et al (2018) Association between bacteria occurring in the apical canal system and expression of bone-resorbing

mediators and matrix metalloproteinases in apical periodontitis. Int Endod J 51(7):738–746
6. Wan C et al (2014) MMP9 deficiency increased the size of experimentally induced apical periodontitis. J Endod 40(5):658–664
7. Herrera BS et al (2011) iNOS-derived nitric oxide stimulates osteoclast activity and alveolar bone loss in ligature-induced periodontitis in rats. J Periodontol 82(11):1608–1615
8. Braz-Silva PH et al (2019) Inflammatory profile of chronic apical periodontitis: a literature review. Acta Odontol Scand 77(3):173–180
9. Probst M et al (2021) Magnetic resonance imaging as a diagnostic tool for periodontal disease: a prospective study with correlation to standard clinical findings-Is there added value? J Clin Periodontol 48(7):929–948
10. Shahbazian M, Jacobs R (2012) Diagnostic value of 2D and 3D imaging in odontogenic maxillary sinusitis: a review of literature. J Oral Rehabil 39(4):294–300
11. Shahbazian M et al (2015) Comparative assessment of periapical radiography and CBCT imaging for radiodiagnostics in the posterior maxilla. Odontology 103(1):97–104
12. Shahbazian M et al (2014) Comparative assessment of panoramic radiography and CBCT imaging for radiodiagnostics in the posterior maxilla. Clin Oral Investig 18(1):293–300
13. Simuntis R et al (2017) Clinical efficacy of main radiological diagnostic methods for odontogenic maxillary sinusitis. Eur Arch Otorhinolaryngol 274(10):3651–3658
14. Bajoria AA, Sarkar S, Sinha P (2019) Evaluation of odontogenic maxillary sinusitis with cone beam computed tomography: a retrospective study with review of literature. J Int Soc Prev Community Dent 9(2):194–204
15. Chong VF, Fan YF (1998) Comparison of CT and MRI features in sinusitis. Eur J Radiol 29(1):47–54
16. Procacci P et al (2017) Odontogenic orbital abscess: a case report and review of literature. Oral Maxillofac Surg 21(2):271–279
17. Munhoz L et al (2018) Diffusion-weighted magnetic resonance imaging in maxillary sinuses inflammatory diseases: report of three cases and literature review. J Oral Maxillofac Res 9(2):e4
18. Ghobrial GM et al (2016) Odontogenic sinusitis resulting in abscess formation within the optic chiasm and tract: case report and review. J Neuroophthalmol 36(4):393–398
19. Juerchott A et al (2020) In vivo accuracy of dental magnetic resonance imaging in assessing maxillary molar furcation involvement: a feasibility study in humans. J Clin Periodontol 47(7):809–815
20. Ruetters M et al (2019) Dental magnetic resonance imaging for periodontal indication - a new approach of imaging residual periodontal bone support. Acta Odontol Scand 77(1):49–54
21. Juerchott A et al (2020) Comparison of non-contrast-enhanced dental magnetic resonance imaging and cone-beam computed tomography in assessing the horizontal and vertical components of furcation defects in maxillary molars: an in vivo feasibility study. J Clin Periodontol 47(12):1485–1495
22. Timme M et al (2020) Imaging of root canal treatment using ultra high field 9.4T UTE-MRI - a preliminary study. Dentomaxillofac Radiol 49(1):20190183
23. Masthoff M et al (2019) Dental Imaging - a basic guide for the radiologist. Rofo 191(3):192–198
24. Pauwels R et al (2012) Effective dose range for dental cone beam computed tomography scanners. Eur J Radiol 81(2):267–271
25. Zidan M et al (2022) Endodontic working length measurements of premolars and molars in high-resolution dental MRI: a clinical pilot study for assessment of reliability and accuracy. Clin Oral Investig 26(11):6765–6772
26. Hilgenfeld T et al (2022) High-resolution single tooth MRI with an inductively coupled intraoral coil-can MRI compete with CBCT? Invest Radiol 57(11):720–727
27. Probst FA et al (2021) Geometric accuracy of magnetic resonance imaging-derived virtual 3-dimensional bone surface models of the mandible in comparison to computed tomography and cone beam computed tomography: a porcine cadaver study. Clin Implant Dent Relat Res 23(5):779–788
28. Hilgenfeld T et al (2020) Use of dental MRI for radiation-free guided dental implant planning: a prospective, in vivo study of accuracy and reliability. Eur Radiol 30(12):6392–6401
29. Valdec S et al (2021) Comparison of preoperative cone-beam computed tomography and 3D-double echo steady-state MRI in third molar surgery. J Clin Med 10(20):4768. https://doi.org/10.3390/jcm10204768
30. Juerchott A et al (2020) In vivo comparison of MRI- and CBCT-based 3D cephalometric analysis: beginning of a non-ionizing diagnostic era in craniomaxillofacial imaging? Eur Radiol 30(3):1488–1497
31. Orstavik D, Kerekes K, Eriksen HM (1986) The periapical index: a scoring system for radiographic assessment of apical periodontitis. Endod Dent Traumatol 2(1):20–34
32. Estrela C et al (2008) A new periapical index based on cone beam computed tomography. J Endod 34(11):1325–1331
33. Gurhan C et al (2020) Evaluation of factors affecting the association between thickening of sinus mucosa and the presence of periapical lesions using cone beam CT. Int Endod J 53(10):1339–1347
34. Shanbhag S et al (2013) Association between periapical lesions and maxillary sinus mucosal thickening: a retrospective cone-beam computed tomographic study. J Endod 39(7):853–857
35. Maillet M et al (2011) Cone-beam computed tomography evaluation of maxillary sinusitis. J Endod 37(6):753–757
36. Van der Cruyssen F et al (2021) Magnetic resonance neurography of the head and neck: state of the art, anatomy, pathology and future perspectives. Br J Radiol 94(1119):20200798
37. Van der Cruyssen F et al (2021) 3D Cranial nerve imaging, a novel MR neurography technique using black-blood STIR TSE with a pseudo steady-state sweep and motion-sensitized driven equilibrium pulse for the visualization of the extraforaminal cranial nerve branches. AJNR Am J Neuroradiol 42(3):578–580
38. Casselman J et al (2022) 3D CRANI, a novel MR neurography sequence, can reliable visualise the extraforaminal cranial and occipital nerves. Eur Radiol 33(4):2861–2870. https://doi.org/10.1007/s00330-022-09269-2
39. Juerchott A et al (2022) Quantitative assessment of contrast-enhancement patterns of the healthy dental pulp by magnetic resonance imaging: a prospective in vivo study. Int Endod J 55(3):252–262
40. Huber FA et al (2020) Medication-related osteonecrosis of the jaw-comparison of bone imaging using ultrashort echo-time magnetic resonance imaging and cone-beam computed tomography. Invest Radiol 55(3):160–167
41. Schumann P et al (2022) Correlation of dynamic contrast-enhanced bone perfusion with morphologic ultra-short echo time MR imaging in medication-related osteonecrosis of the jaw. Dentomaxillofac Radiol 51(2):20210036
42. Jimenez-Boj E et al (2007) Bone erosions and bone marrow edema as defined by magnetic resonance imaging reflect true bone marrow inflammation in rheumatoid arthritis. Arthritis Rheum 56(4):1118–1124
43. Baraliakos X et al (2005) Assessment of acute spinal inflammation in patients with ankylosing spondylitis by magnetic resonance imaging: a comparison between contrast enhanced T1 and short tau inversion recovery (STIR) sequences. Ann Rheum Dis 64(8):1141–1144
44. Newbould RD et al (2017) T2 relaxation mapping MRI of healthy and inflamed gingival tissue. Dentomaxillofac Radiol 46(2):20160295

Authors and Affiliations

Egon Burian[1,2,3] · Georg Feuerriegel[3] · Nico Sollmann[1,2,4] · Gintare Burian[5] · Benjamin Palla[6] · Magdalena Griesbauer[1] · Caspar Bumm[7] · Monika Probst[1] · Meinrad Beer[2] · Matthias Folwaczny[7]

Georg Feuerriegel
g.feuerriegel@tum.de

Nico Sollmann
nico.sollmann@tum.de

Gintare Burian
gintare.burian@med.uni-muenchen.de

Benjamin Palla
palla1@uic.edu

Magdalena Griesbauer
lena@der-griesbauer.de

Caspar Bumm
caspar.bumm@med.uni-muenchen.de

Monika Probst
monika.probst@tum.de

Meinrad Beer
meinrad.beer@uniklinik-ulm.de

Matthias Folwaczny
matthias.folwaczny@med.uni-muenchen.de

[1] Department of Diagnostic and Interventional Neuroradiology, Klinikum Rechts Der Isar, School of Medicine, Technical University of Munich, Munich, Germany

[2] Department of Diagnostic and Interventional Radiology, University Hospital Ulm, Ulm, Germany

[3] Department of Diagnostic and Interventional Radiology, Klinikum Rechts Der Isar, School of Medicine, Technical University of Munich, Ismaninger Str. 22, 81675 Munich, Germany

[4] TUM-Neuroimaging Center, Klinikum Rechts Der Isar, Technical University of Munich, Munich, Germany

[5] Department of Prosthodontics, LMU University Hospital, Ludwig-Maximilians-University, Munich, Germany

[6] Department of Oral and Maxillofacial Surgery, University of Illinois, Chicago, IL, USA

[7] Department of Restorative Dentistry and Periodontology, LMU University Hospital, Munich, Germany